Mono- *versus* Binuclear Zn-Carbamodithioate Complexes as Efficient Homogeneous Catalysts for the Cycloaddition of Epoxides with CO_2

Feda'a M. Al-Qaisi,[a*] Abdussalam K. Qaroush,[b*] Ahmad M. Ala'mar,[a] Ala'a F. Eftaiha,[a*] Khaleel I. Assaf,[c] and Timo Repo[a,d]

[a] Department of Chemistry, Faculty of Science, The Hashemite University, Zarqa 13133, Jordan
[b] Department of Chemistry, Faculty of Science, The University of Jordan, Amman 11942, Jordan
[c] Department of Chemistry, Faculty of Science, Al-Balqa Applied University, Al-Salt 19117, Jordan
[d] Department of Chemistry, University of Helsinki, A.I. Virtasen aukio 1, 00014 Helsinki, Finland

Corresponding authors E-mails: fedaam@hu.edu.jo, a.qaroush@ju.edu.jo, alaa.eftaiha@hu.edu.jo

Electronic Supplementary Information

Table of Content

*1. Characterization of compound **3***

Upon quaternization of **2**, the chemical shifts of the imidazole head and base protons (H1, H2 and H3) were downfielded from 7.58, 7.09 and 6.92 to 9.17, 7.80 and 7.73 ppm, respectively (**Figure S1**). In addition, propylene chain protons with the most prominent downfield peak of H5 with a chemical shift from 3.54 to 4.24 ppm as a result of quaternization. In parallel, H6 and H7 influenced slightly shifted from 2.36, 3.70 to 2.15, 3.60 ppm, respectively. The ^{1}H NMR spectrum of **3** (400 MHz, DMSO-d_6) is summarized as follows: δ 9.17 (s, 1H), 7.87 (m, 4H), 7.80 (t, 1H), 7.73 (t, 1H), 4.24 (t, 2H), 3.86 (s, 3H), 3.60 (t, 2H), 2.15 (m, 2H). Alongside, ^{13}C NMR chemical shift showed clear evidence for the change in chemical shifts within the imidazole carbons (C1, C2, C3 and C4) from 138.1, 128.4, 120.5 and 32.3 to 136.8, 123.6, 122.3 and 35.8 ppm, respectively. Likewise, alkyl chain carbons (C5, C6 and C7) after imidazolium formation changing from 31.8, 31.1 and 36.1 to 34.2, 28.6 and 46.5 ppm, respectively. Furthermore, ATR-FTIR analysis (**Figure S2**) confirmed quaternization with a blue shift in **2** (C=N, C-N) peaks from 1610, 1080 to 1631, 1165 cm^{-1} in **3** (C=N^{+}, C-N^{+}), and a red shift in C-H starching peak from 3106 to 3045 cm^{-1}.[1]

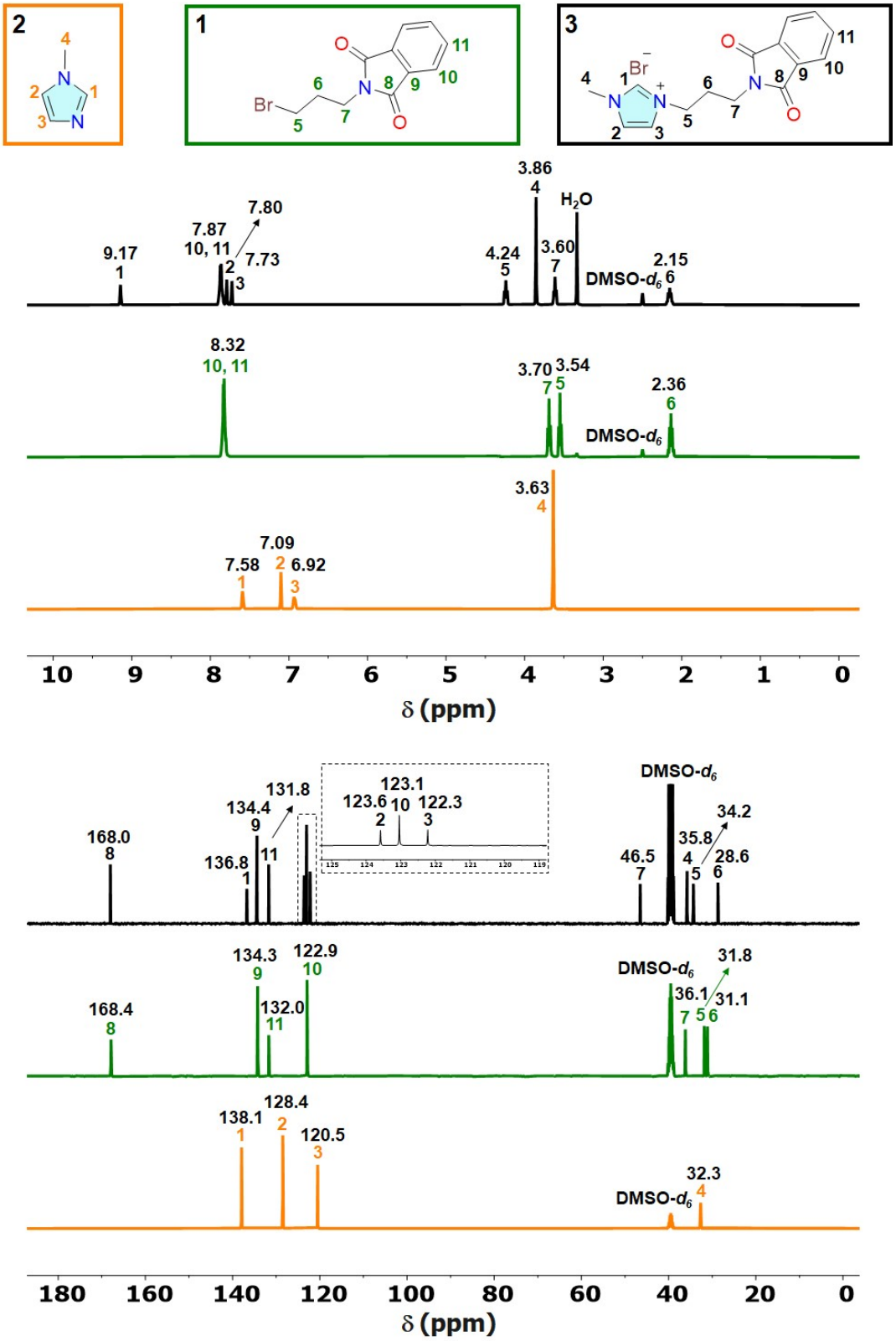

Figure S1 . $^{1}H/^{13}C$ NMR spectra of compounds **1-3** measured in DMSO-d_6.

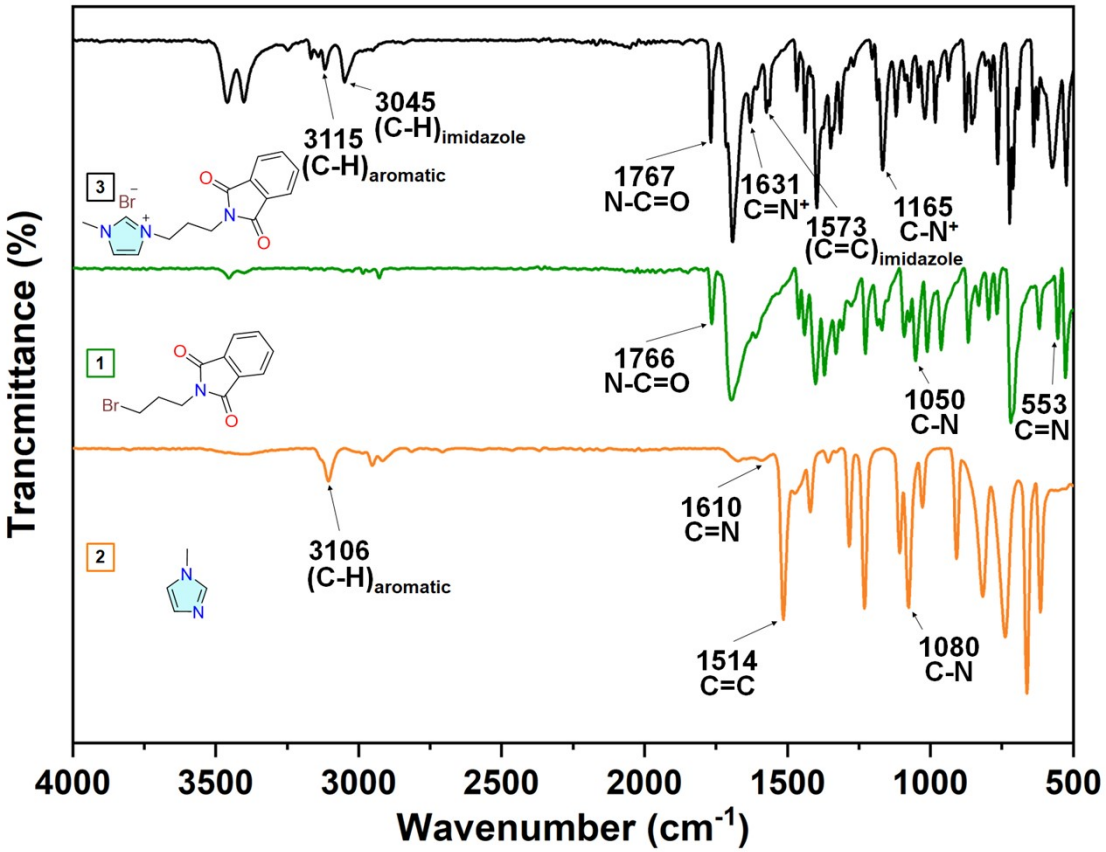

Figure S2. ATR-FTIR spectra of compounds **1**-**3** measured in the solid state.

2. *Characterization of compound **4***

Compound **4** was obtained *via* acidic hydrolysis of **3** with HBr in H_2O and glacial AcOH. The ^{1}H NMR spectrum (**Figure S3**) shows the appearance of a new peak corresponding to $–NH_3^+$ at 7.98 ppm, the disappearance of the phthalimide protons (H8), slight downfield shifts of imidazolium protons from 9.17, 7.80 and 7.73 to 9.24, 7.84 and 7.75 ppm, respectively and an upfield chemical shift of H6, located closest to the ammonium moiety, from 3.60 to 2.82 ppm. Moreover, the ^{13}C NMR analysis (**Figure S3**) confirm the disappearance of carbons C8-11, supporting the hydrolysis of the phthalimide group, and the chemical shifts in propyl chain (C4-6) and the methyl group (C7) attached to the imidazolium ring shift from 46.5, 28.6, 35.8 and 34.2 to 45.9, 27.5, 35.9 and 35.7 ppm, respectively. *Ex situ* ATR-FTIR spectra (**Figure S4**) confirm the hydrolysis of imide (O=C-

N-C=O) peak at 1767 cm^{-1}, and appearance of new (a)symmetric-stretching peaks, bending and rocking bands corresponding to the terminal ammonium group ($-NH_3^+$).[2]

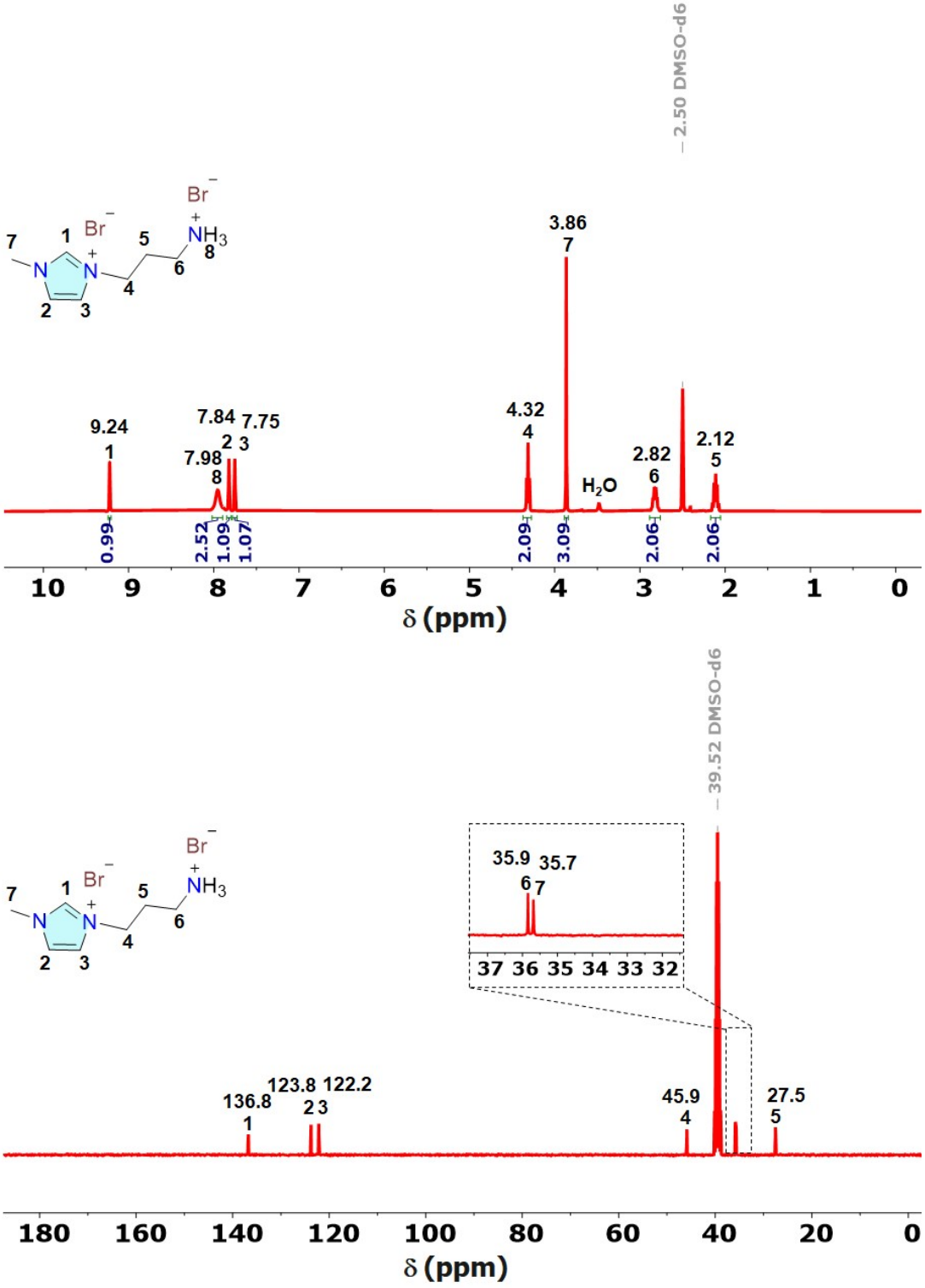

Figure S3 . $^{1}H/^{13}C$ NMR spectra of compound **4** in DMSO-d_6.

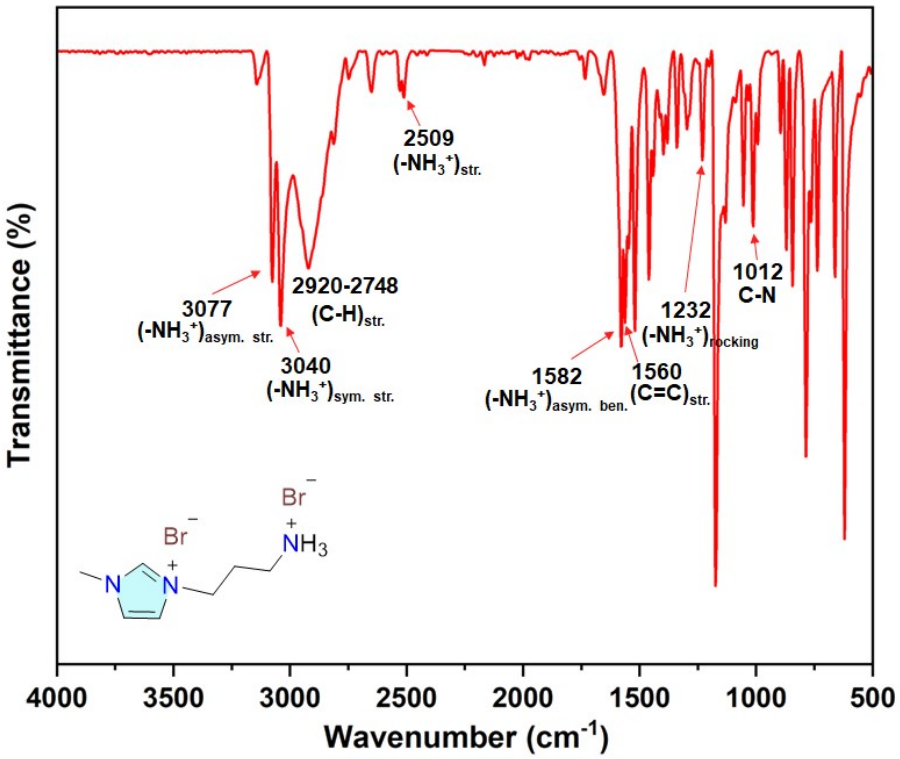

Figure S4. ATR-FTIR spectrum of **4** in the solid state.

*3. Synthesis and characterization of compound **8***

The synthesis of **8** was performed following a previously reported task-specific ionic liquid (TSIL) procedure reported by our research group.[2] Sodium hydride (NaH, 0.82 g, 0.021 mol) was suspended in 30 mL of anhydrous THF, and stirred for 15 min in an ice bath, which was then added to a solution of imidazole (**7**; 1.22 g, 0.018 mol) dissolved in 20 mL of anhydrous THF. The mixture was stirred at 0 °C for 1 h.

A solution of N-(3-bromopropyl) phthalimide (**1**; 10.55 g, 0.039 mol) in 30 mL of anhydrous THF was added to the reaction mixture, which was stirred at RT for 1 h. The mixture was then refluxed for 72 h at 80 °C with continuous stirring. Upon cooling to RT, a white precipitate formed, which was filtered and washed with 100 mL of THF. The product was recrystallized from hot EtOH to remove sodium bromide (NaBr). Yield: 90%. Melting point (°C) = 235 °C (not corrected).

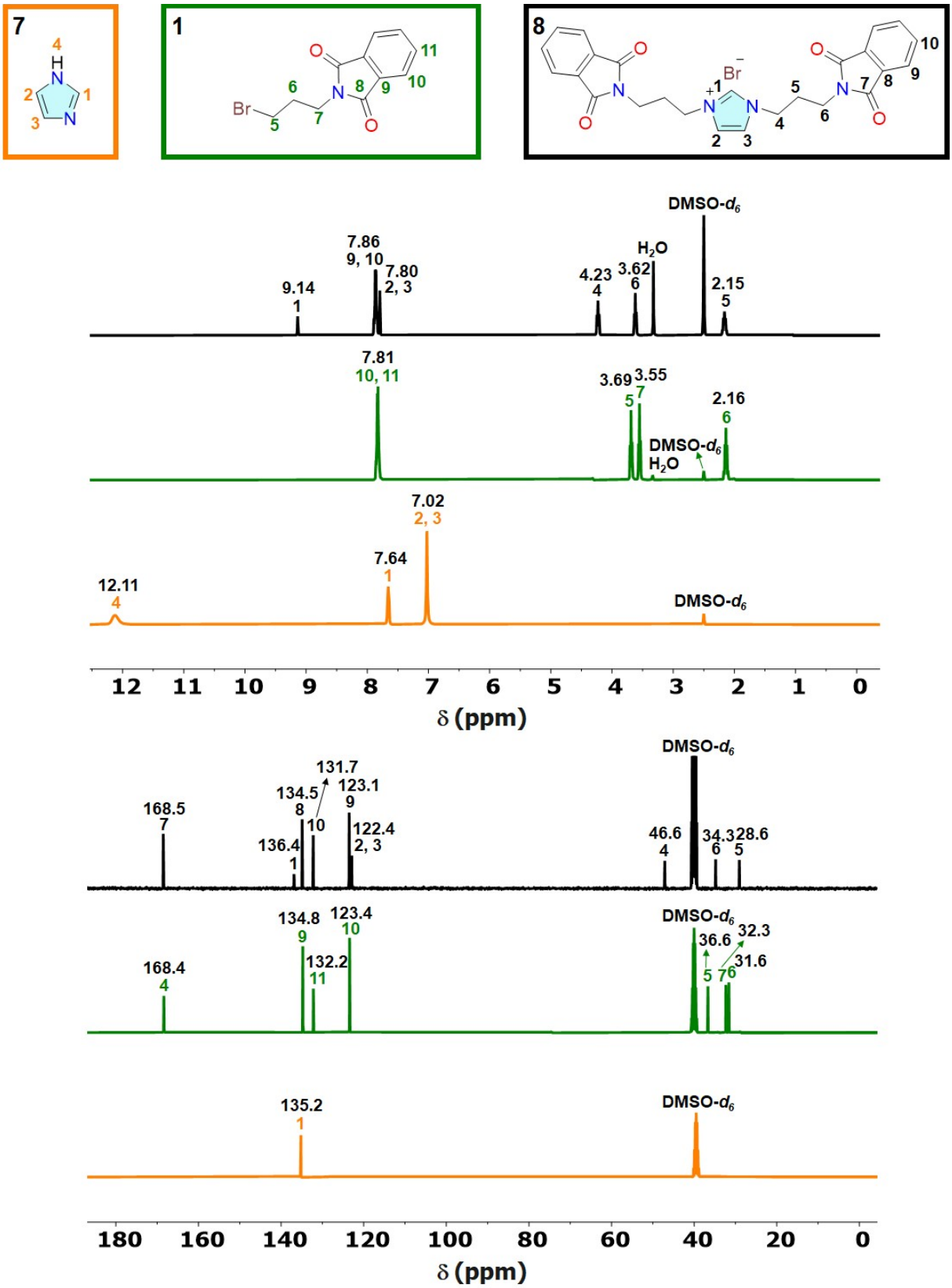

Figure S5. $^{1}H/^{13}C$ NMR spectra of compounds **1**, **7** and **8** measured in DMSO-d_6.

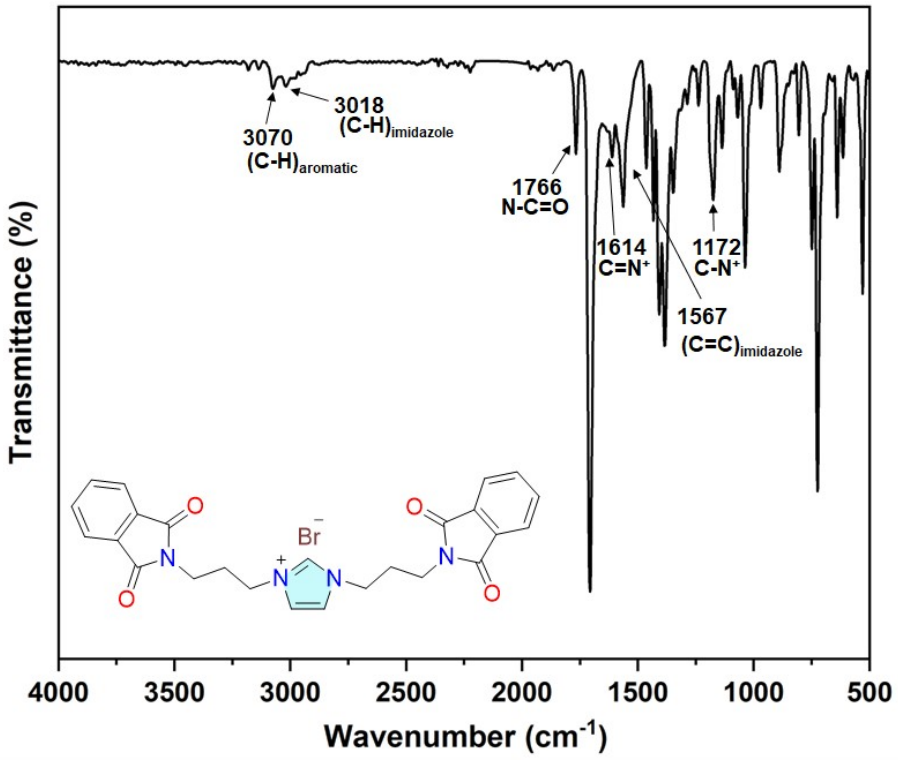

Figure S6. ATR-FTIR spectrum of **8** in the solid state.

*4. Synthesis and characterization of compound **9***

The TSIL precursor (**8**, 2 g, 5.71 mmol) was dissolved in a mixture of glacial acetic acid (20 mL) and HBr (20 ml). The solution was refluxed at 110 °C for 24 h, then the solvent was evaporated to yield a brown solid. The crude product was soaked in 30 mL of acetone, followed by decantation of the brownish solution to remove phthalic acid. The process was repeated twice, producing a white solid (**9**), which was dried under vacuum with yield up to 87%. Melting point = 215 ℃ (not corrected).

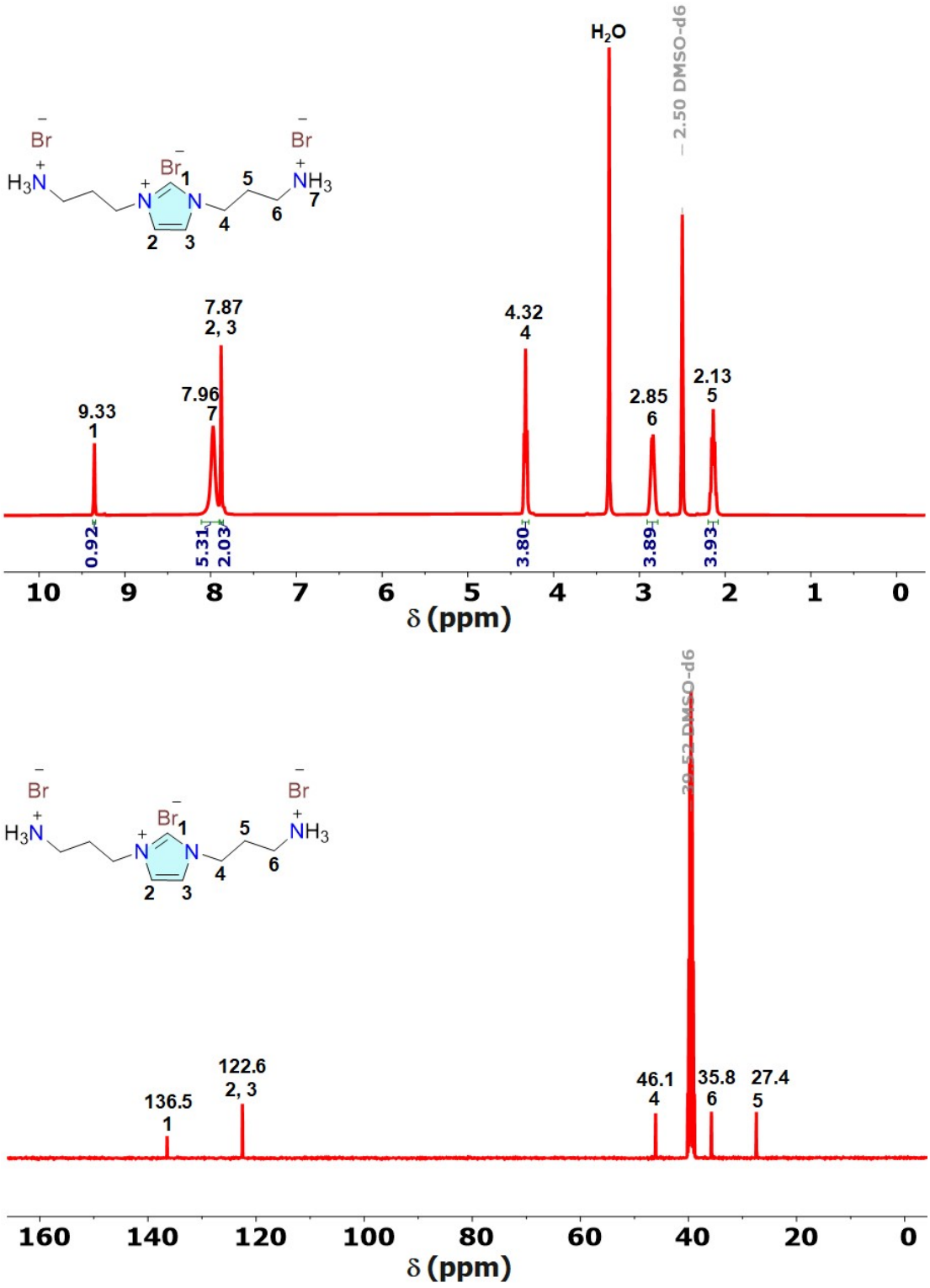

Figure S7 . $^{1}H/^{13}C$ NMR spectra of compound **9** in DMSO-d_6.

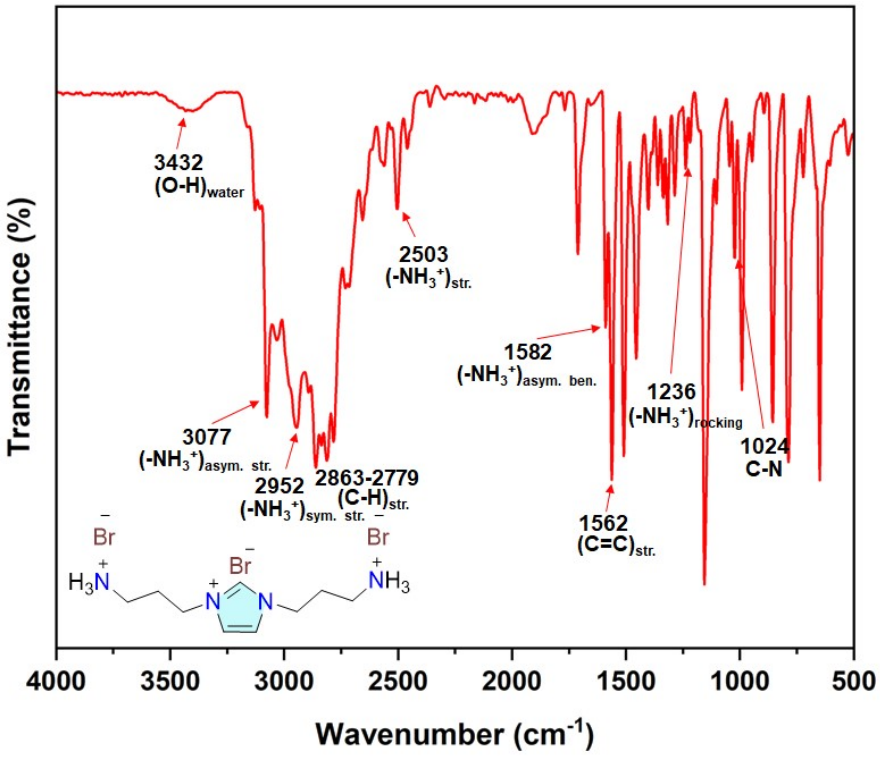

Figure S8. ATR-FTIR spectrum of **9** in the solid state.

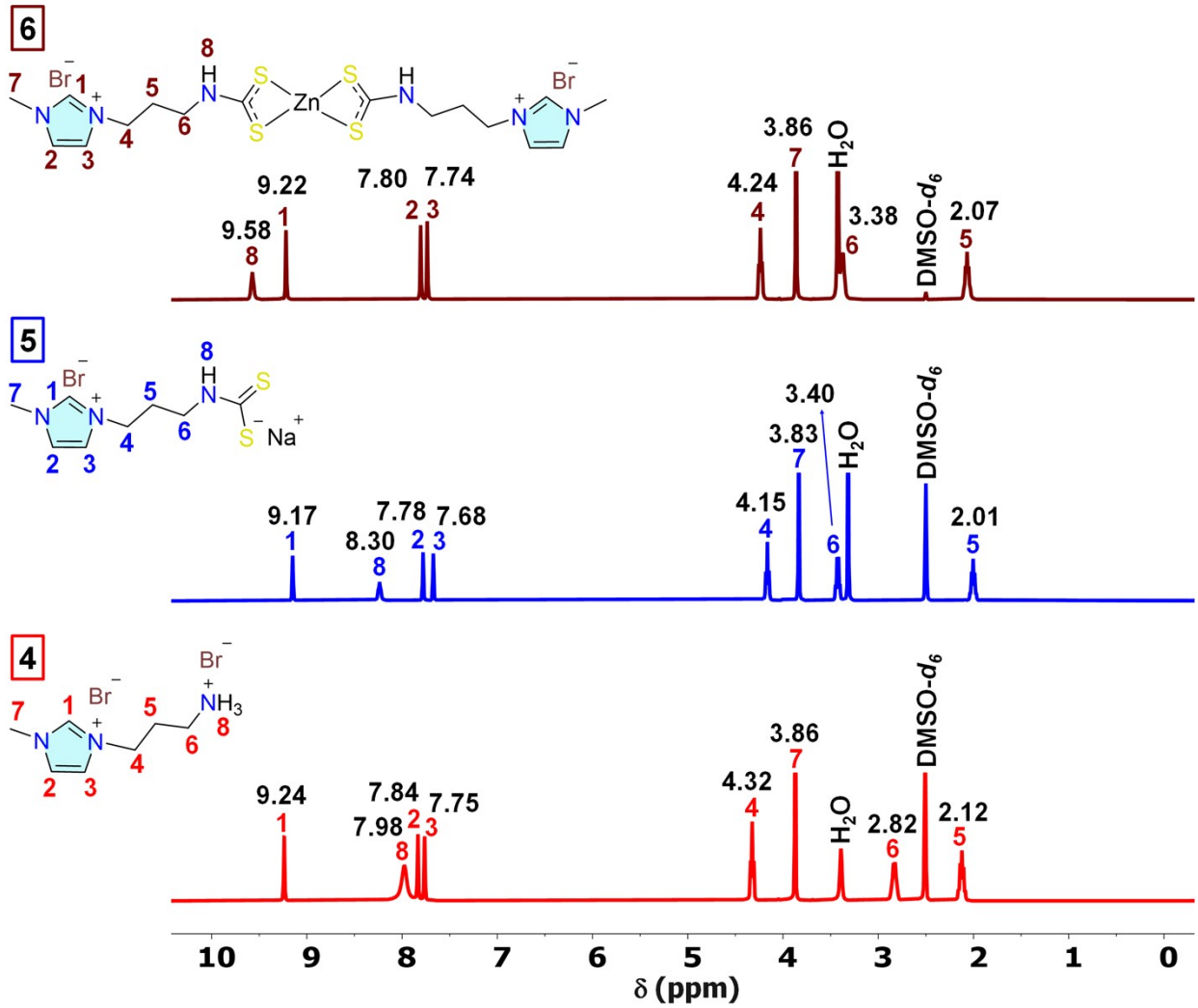

Figure S9. ^{1}H NMR spectra of compounds **4** (red trace), **5** (blue trace) and **6** (maroon trace) in DMSO-d_6.

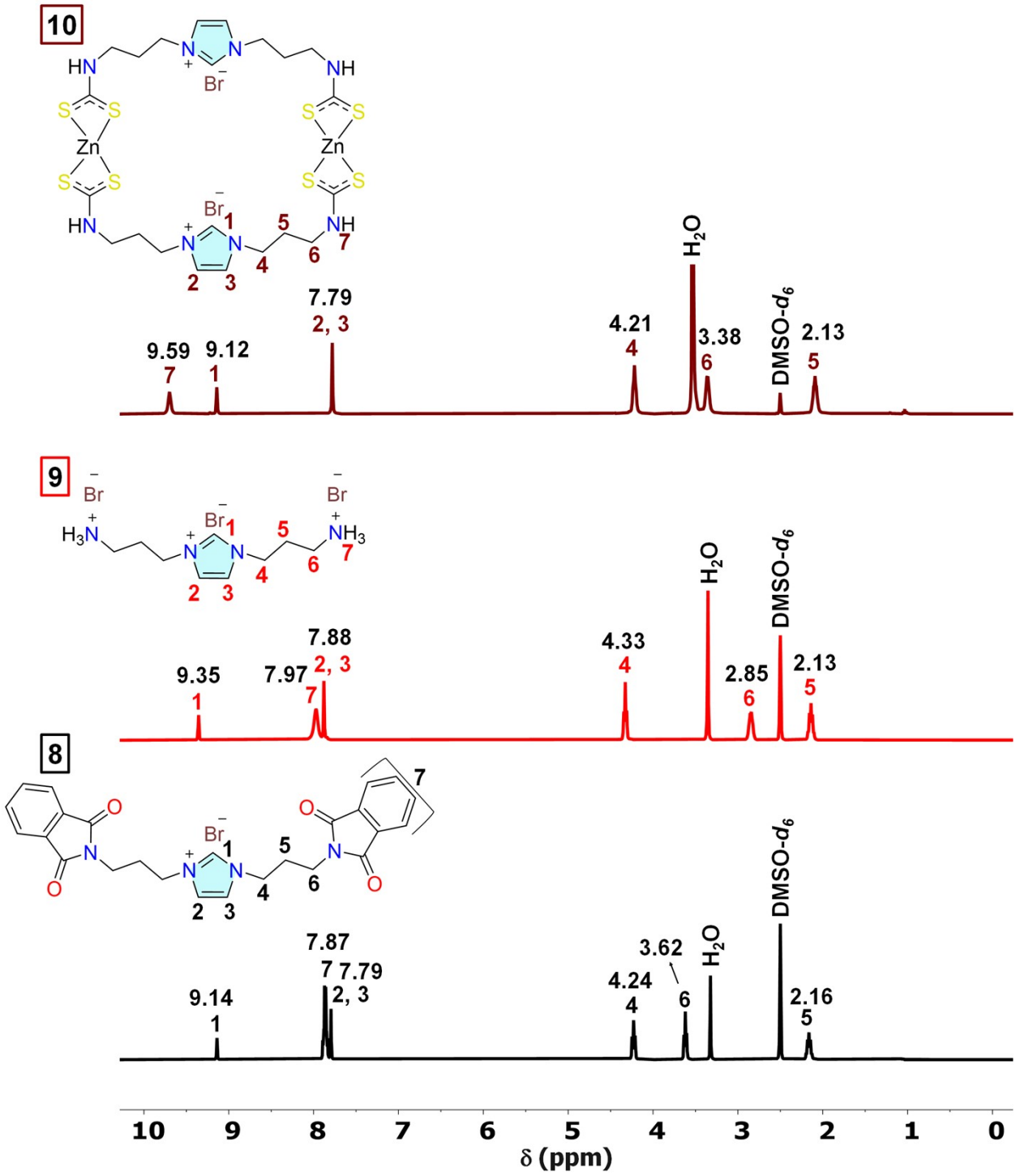

Figure S10. ^{1}H NMR spectra of compounds of **8** (black trace), **9** (red trace) and **10** (maroon trace) in DMSO-d_6. X_1: EtOH, X_2: Et_2O.

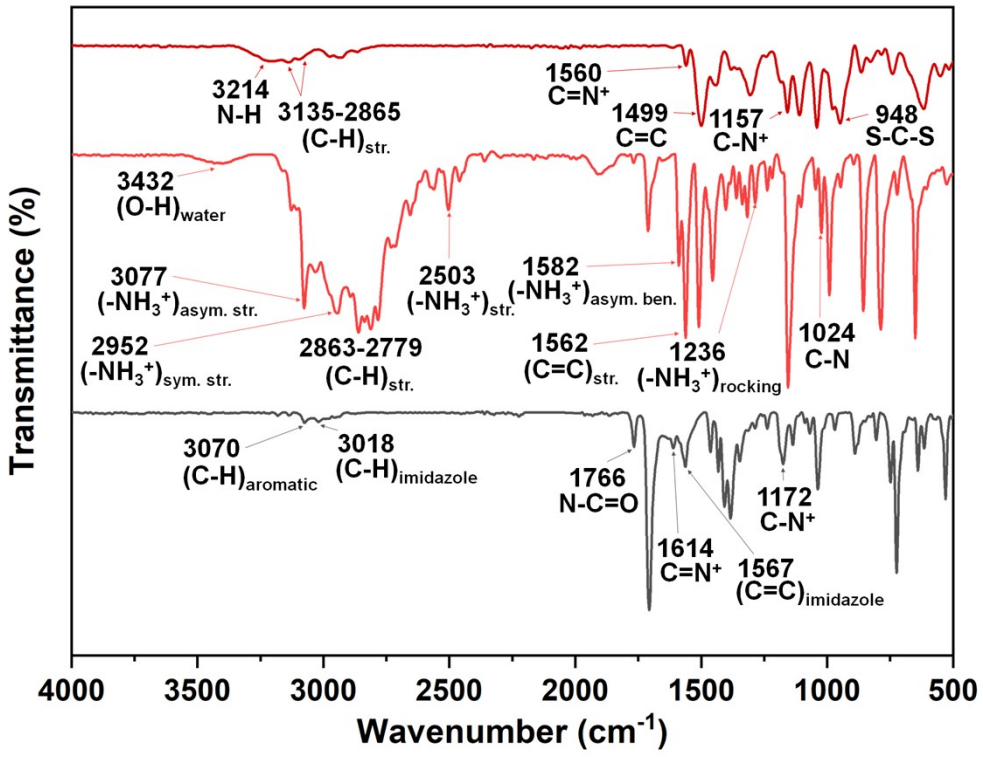

Figure S11. ATR-FTIR spectra of **8** (black), **9** (red) and **10** (maroon) in the solid state.

5. Cycloaddition reactions

5.1. Optimization the reaction condition using ECH

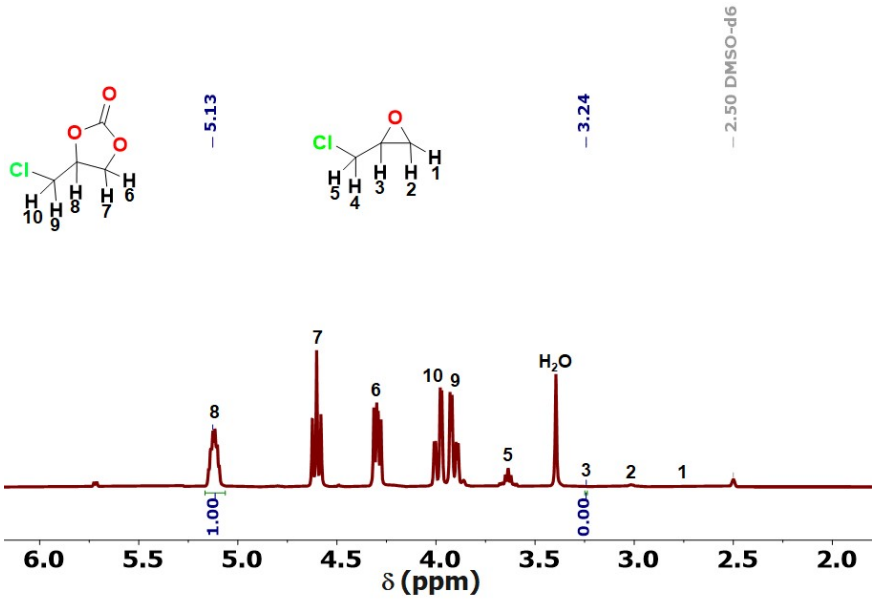

Figure S 12. ^{1}H NMR spectrum (measured in DMSO-d_6) of the conversion of ECH into the 4-chloromethyl-2-oxo-1,3-dioxolane catalyzed by 1 mol% Zn-dtc$_2$ in 0.2 mL DMSO-d_6,1 atm CO_2 (balloon) and 80 °C for 8 h (Entry 1, Table 1).

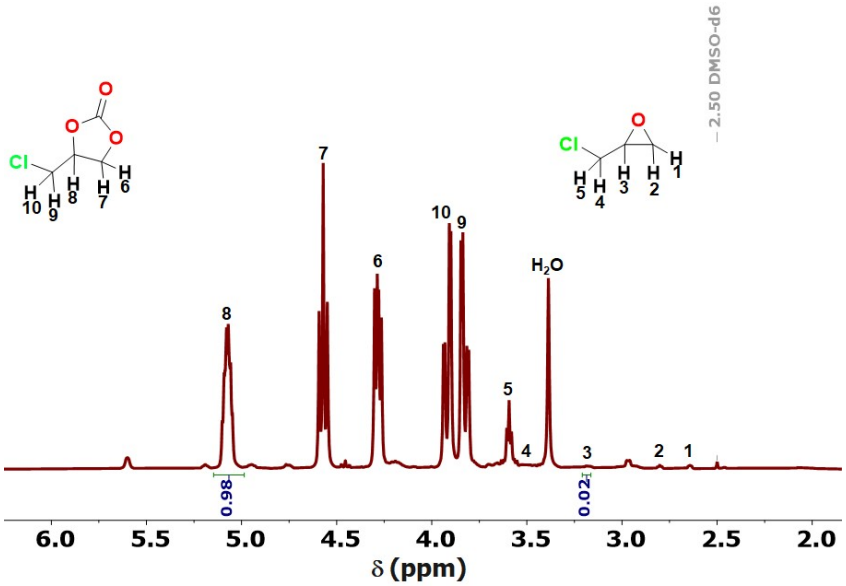

Figure S13. ^{1}H NMR spectrum (measured in DMSO-d_6) of the conversion of ECH into the 4-chloromethyl-2-oxo-1,3-dioxolane catalyzed by 1 mol% Zn-dtc$_2$ in 0.2 mL DMSO-d_6,1 atm CO_2 (balloon) and 80 °C for 4 h (Entry 2, Table 1).

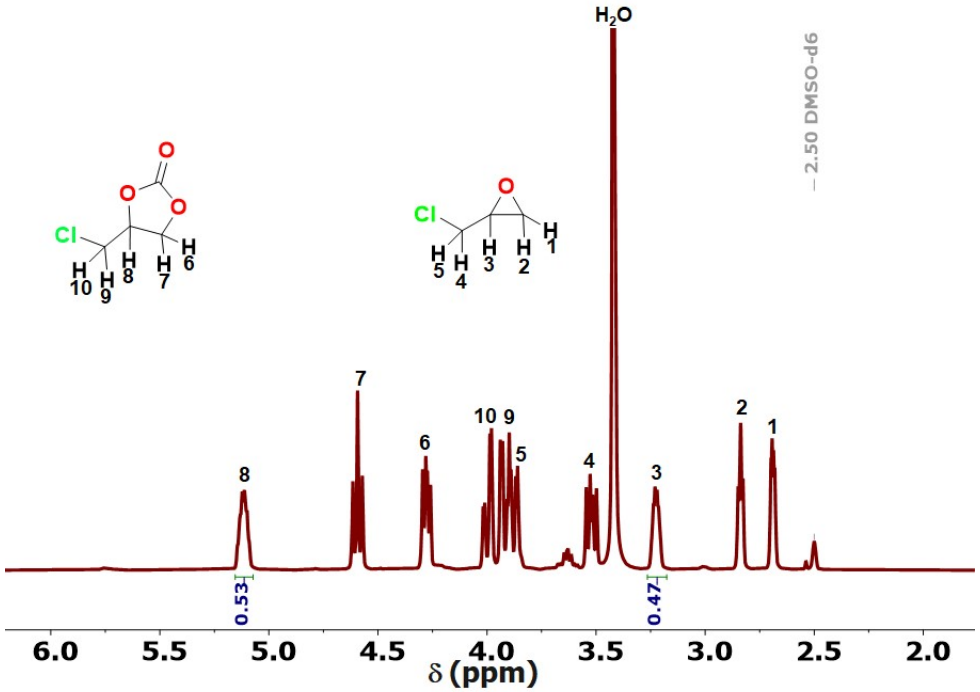

Figure S14. ^{1}H NMR spectrum (measured in DMSO-d_6) of the conversion of ECH into the 4-chloromethyl-2-oxo-1,3-dioxolane catalyzed by 1 mol% Zn-dtc$_2$ in 0.2 mL DMSO-d_6,1 atm CO_2 (balloon) and 80 °C for 2 h (Entry 3, Table 1).

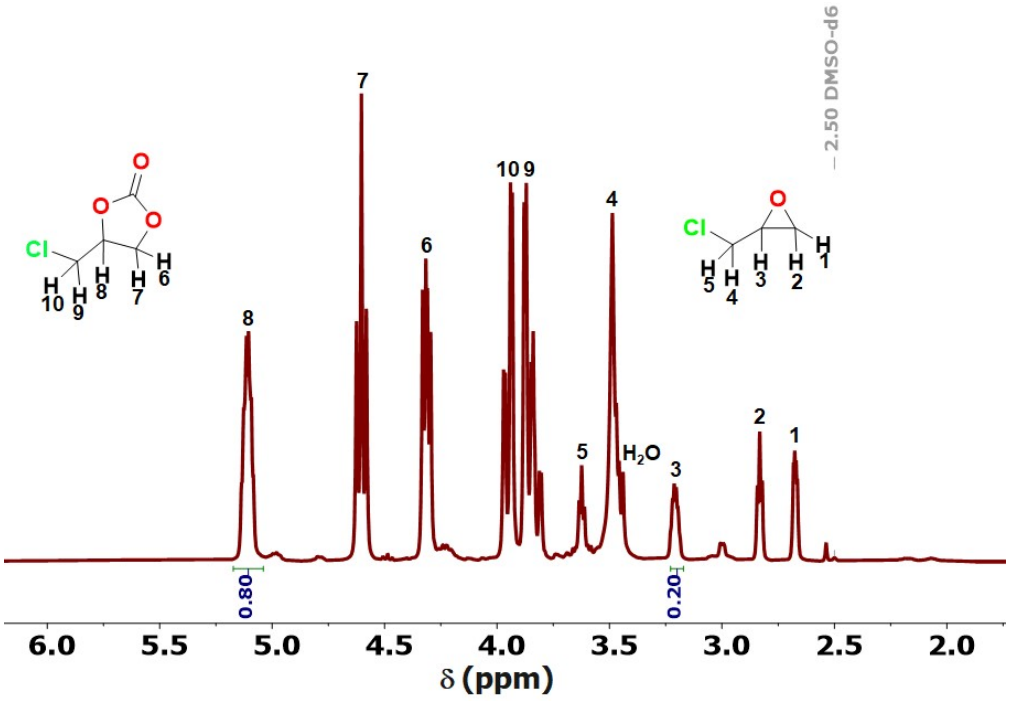

Figure S15. [1]H NMR spectrum (measured in DMSO-d_6) of the conversion of ECH into the 4-chloromethyl-2-oxo-1,3-dioxolane catalyzed by 1 mol% Zn-dtc$_2$ in 0.2 mL DMSO-d_6, 1 atm CO_2 (balloon) and 60 °C for 4 h (Entry 4, Table 1).

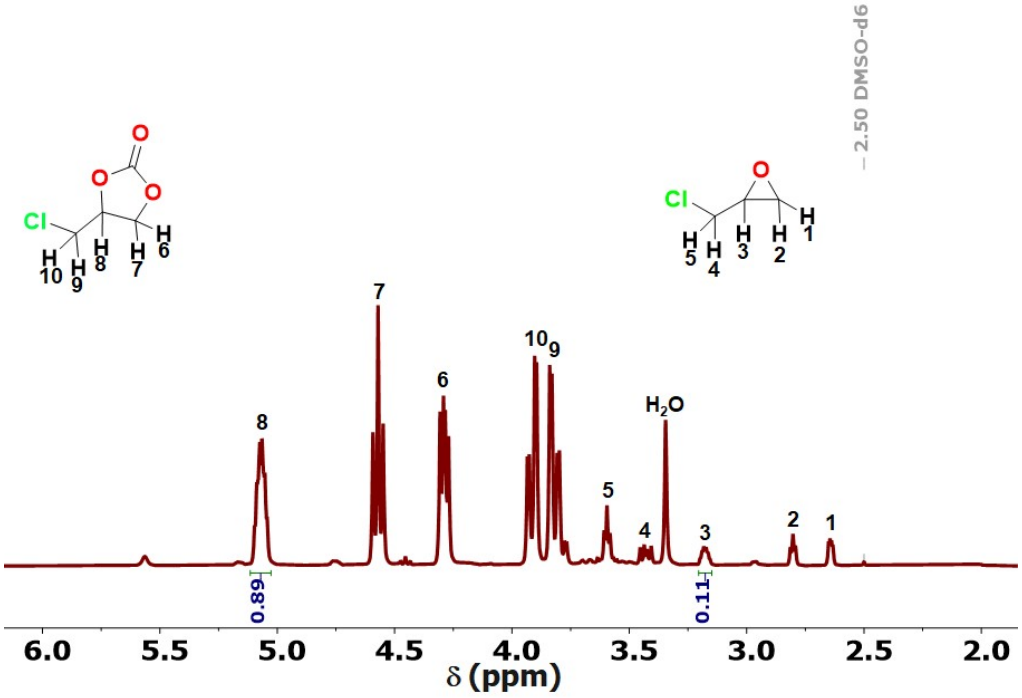

Figure S16. [1]H NMR spectrum (measured in DMSO-d_6) of the conversion of ECH into the 4-chloromethyl-2-oxo-1,3-dioxolane catalyzed by 0.5 mol% Zn-dtc$_2$ in 0.2 mL DMSO-d_6, 1 atm CO_2 (balloon) and 80 °C for 4 h (Entry 5, Table 1).

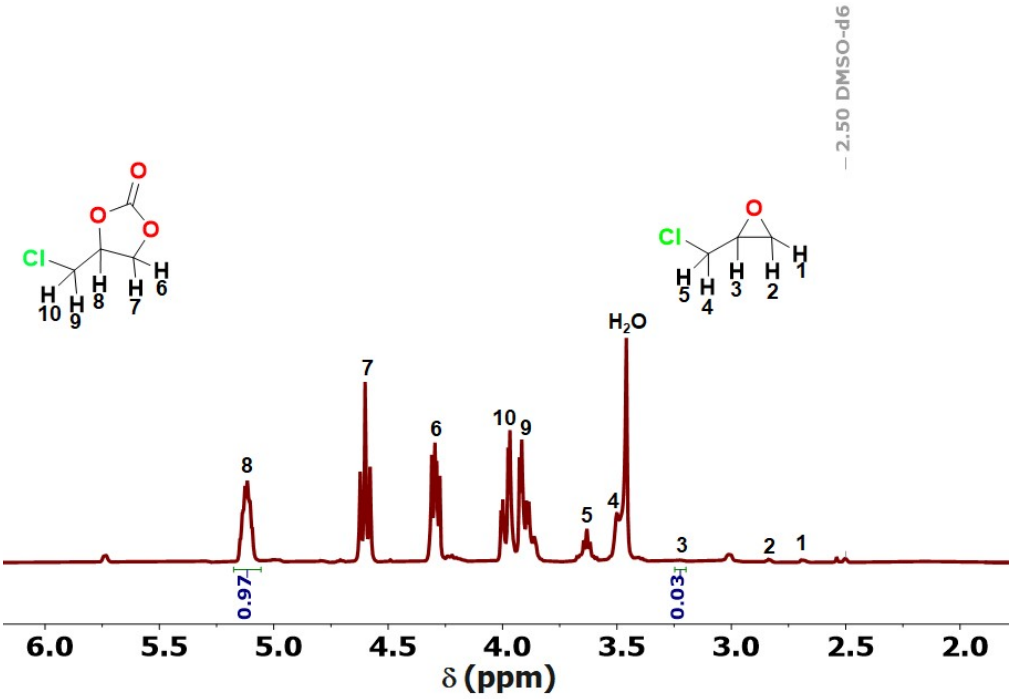

Figure S17. [1]H NMR spectrum (measured in DMSO-d_6) of the conversion of ECH into the 4-chloromethyl-2-oxo-1,3-dioxolane catalyzed by 1.5 mol% Zn-dtc$_2$ in 0.2 mL DMSO-d_6, 1 atm CO_2 (balloon) and 60 °C for 4 h (Entry 6, Table 1).

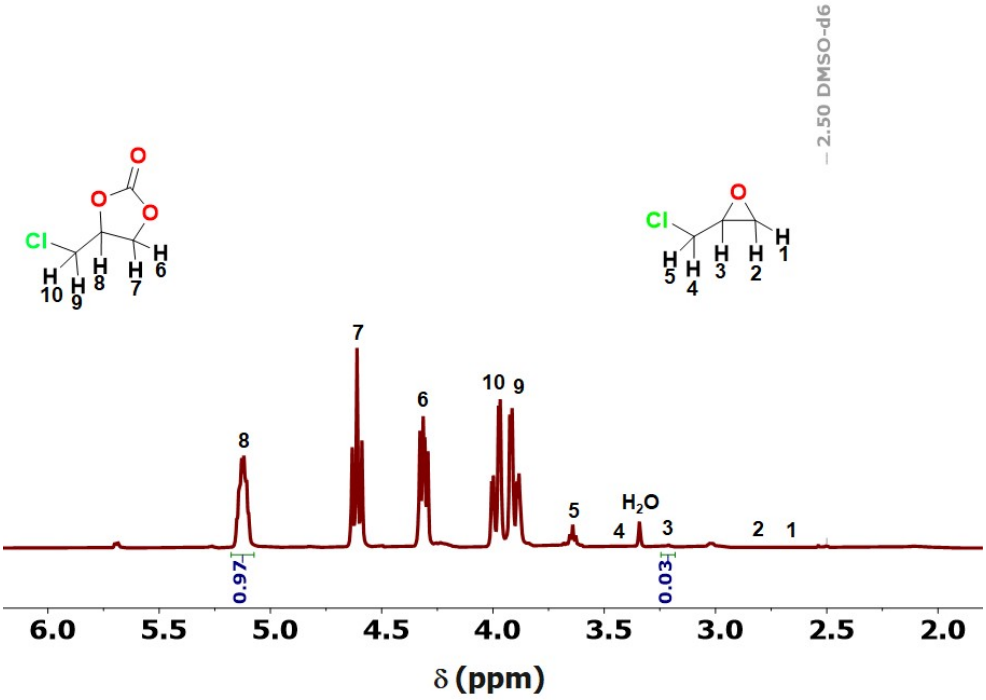

Figure S18. [1]H NMR spectrum (measured in DMSO-d_6) of the conversion of ECH into the 4-chloromethyl-2-oxo-1,3-dioxolane catalyzed by 1 mol% Zn-dtc$_2$ in neat condition, 1 atm CO_2 (balloon) and 80 °C for 4 h (Entry 7, Table 1).

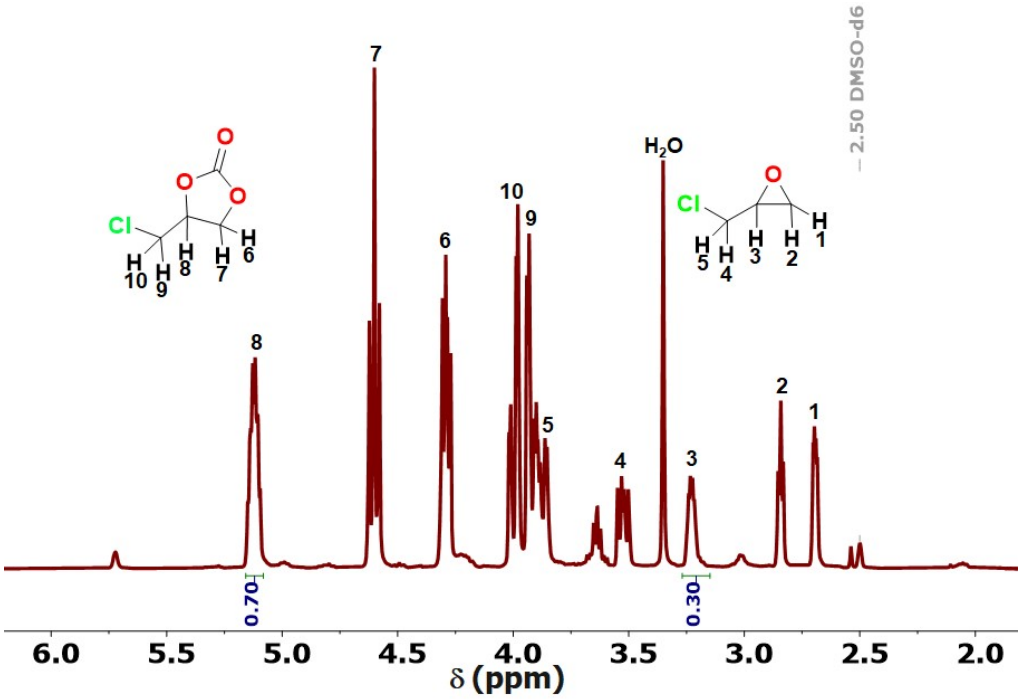

Figure S19. [1]H NMR spectrum (measured in DMSO-d_6) of the conversion of ECH into the 4-chloromethyl-2-oxo-1,3-dioxolane catalyzed by 1 mol% Zn-dtc$_2$ in neat condition, 1 atm CO_2 (balloon) and 80 °C for 2 h (Entry 8, Table 1).

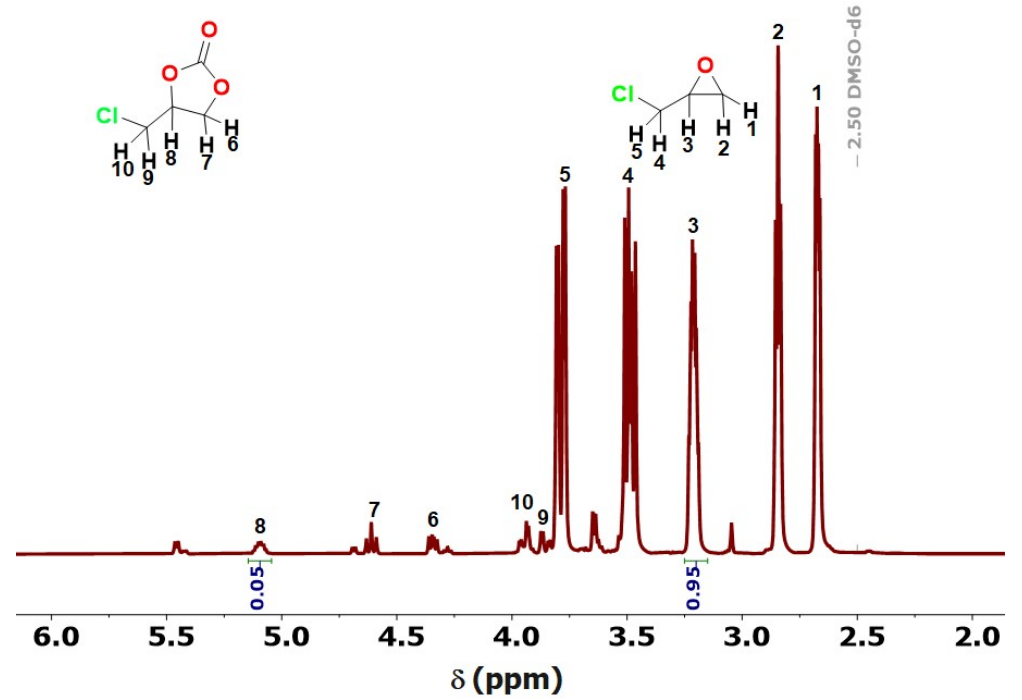

Figure S20. [1]H NMR spectrum (measured in DMSO-d_6) of the conversion of ECH into the 4-chloromethyl-2-oxo-1,3-dioxolane catalyzed by 1 mol% $ZnBr_2$ in 0.2 mL DMSO-d_6, 1 atm CO_2 (balloon) and 80 °C for 4 h (Entry 9, Table 1).

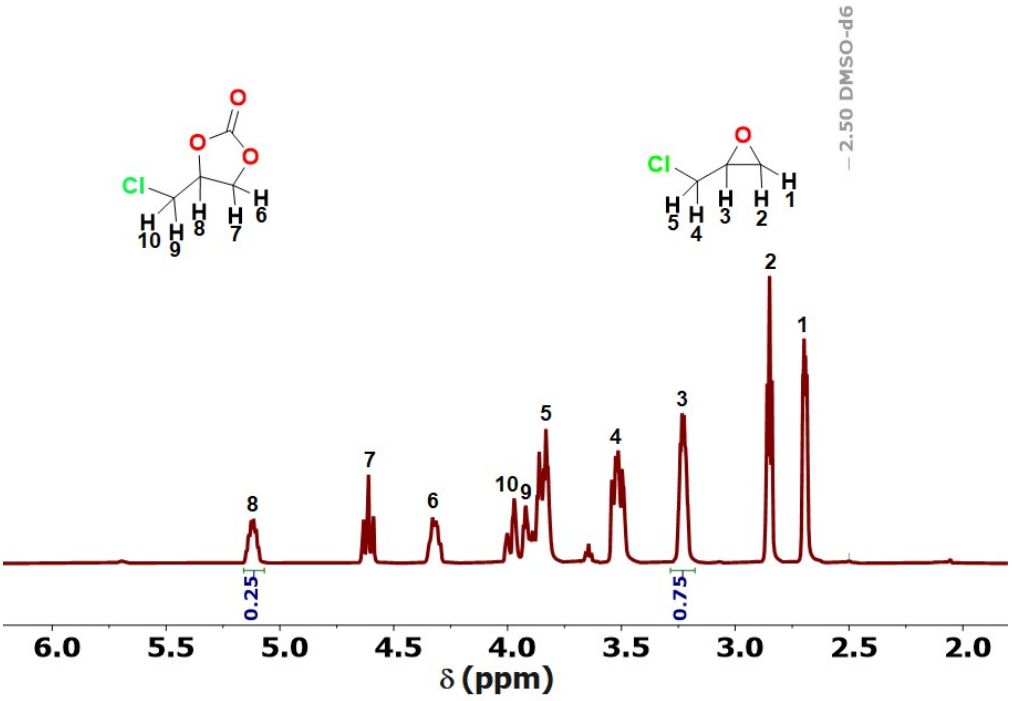

Figure S21. ^{1}H NMR spectrum (measured in DMSO-d_6) of the conversion of ECH into the 4-chloromethyl-2-oxo-1,3-dioxolane catalyzed by 1 mol% dtc in 0.2 mL DMSO-d_6, 1 atm CO_2 (balloon) and 80 °C for 4 h (Entry 10, Table 1).

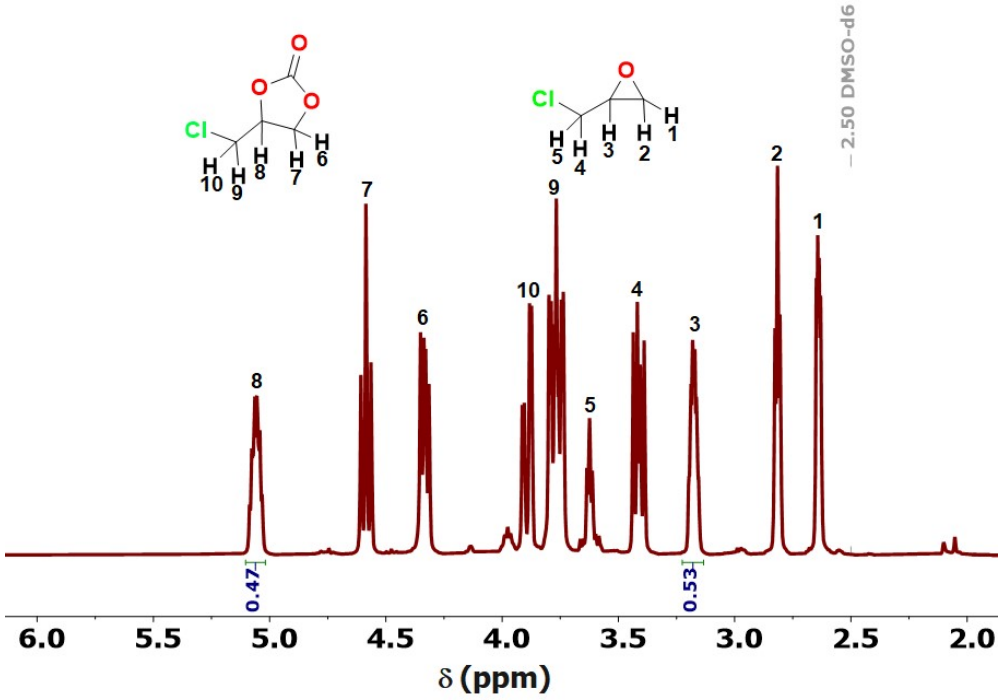

Figure S22. ^{1}H NMR spectrum (measured in DMSO-d_6) of the conversion of ECH into the 4-chloromethyl-2-oxo-1,3-dioxolane catalyzed by 2 mol% dtc in 0.2 mL DMSO-d_6, 1 atm CO_2 (balloon) and 80 °C for 4 h (Entry 11, Table 1).

5.2. Coupling reaction of different epoxides with CO_2 under the optimized reaction conditions

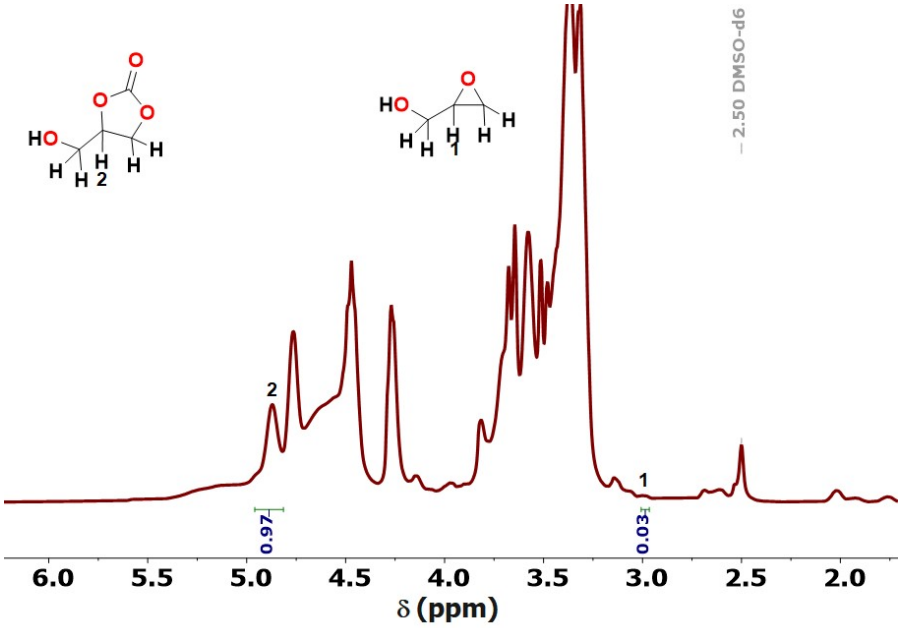

Figure S23. ^{1}H NMR spectrum (measured in DMSO-d_6) of the conversion of GO into the 4-(hydroxymethyl)-1,3-dioxolan-2-one catalyzed by 1 mol% Zn-dtc$_2$ in neat conditions, 1 atm CO_2 (balloon) and 80 °C for 4 h (Entry 2, Table 2).

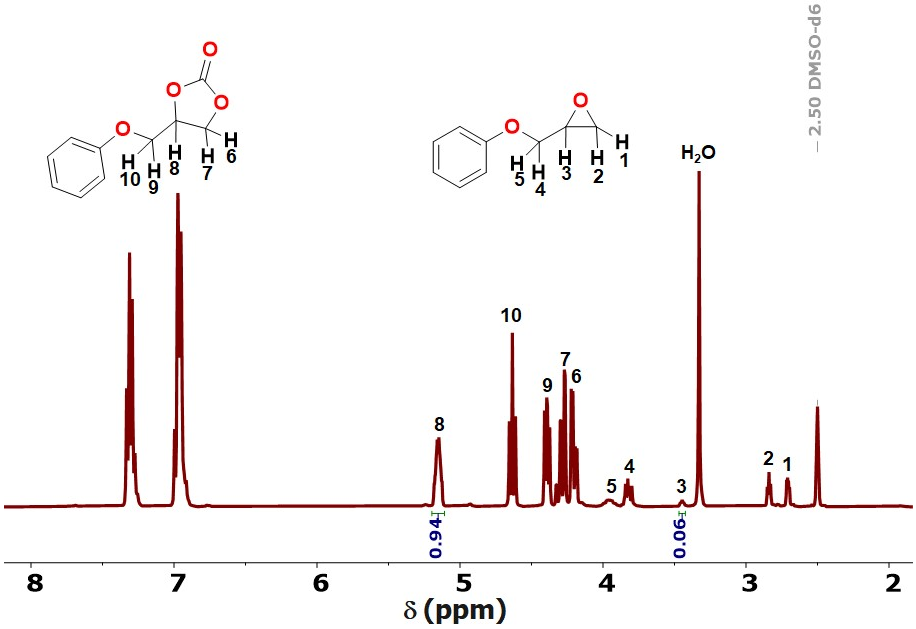

Figure S24. ^{1}H NMR spectrum (measured in DMSO-d_6) of the conversion of POP into the 4-(phenoxymethyl)-1,3-dioxolan-2-one catalyzed by 1 mol% Zn-dtc$_2$ in neat conditions, 1 atm CO_2 (balloon) and 80 °C for 4 h (Entry 3, Table 2).

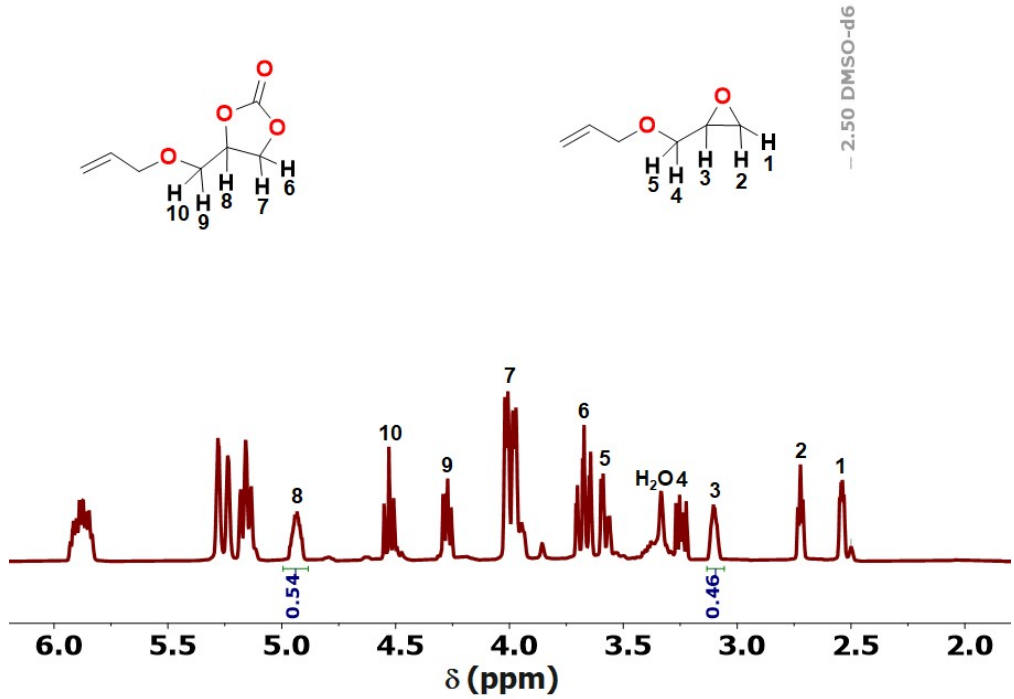

Figure S25. ^{1}H NMR spectrum (measured in DMSO-d_6) of the conversion of AEG into 4-((allyloxy)methyl)-1,3-dioxolan-2-one catalyzed by 1 mol% Zn-dtc$_2$ in neat conditions, 1 atm CO_2 (balloon) and 80 °C for 4 h (Entry 4, Table 2).

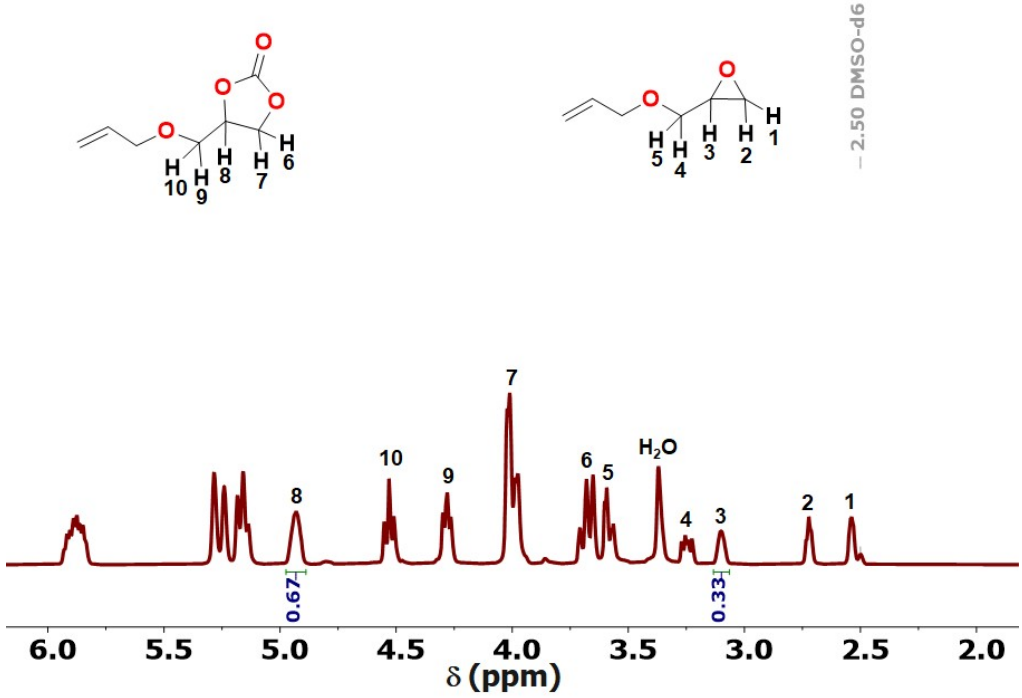

Figure S26. ^{1}H NMR spectrum (measured in DMSO-d_6) of the conversion of AEG into 4-((allyloxy)methyl)-1,3-dioxolan-2-one catalyzed by 1 mol% Zn-dtc$_2$ in 0.2 mL DMSO-d_6, 1 atm CO_2 (balloon) and 80 °C for 4 h (Entry 4, Table 2).

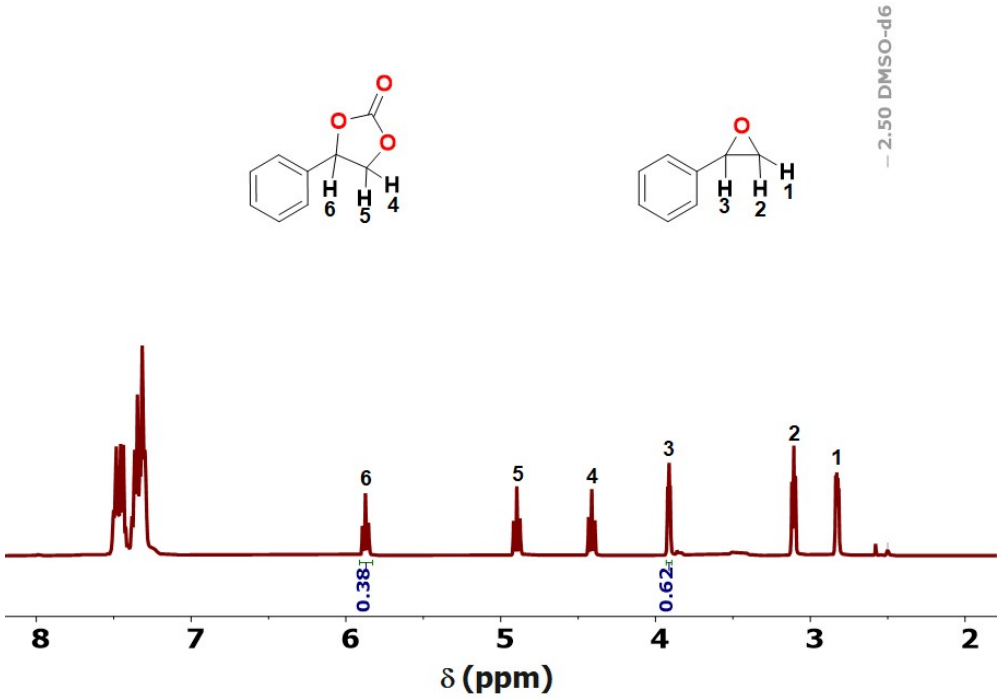

Figure S27. ^{1}H NMR spectrum (measured in DMSO-d_6) of the conversion of SO into the 4-phenyl-1,3-dioxolan-2-one catalyzed by 1 mol% Zn-dtc$_2$ in neat conditions, 1 atm CO_2 (balloon) and 80 °C for 4 h (Entry 5, Table 2).

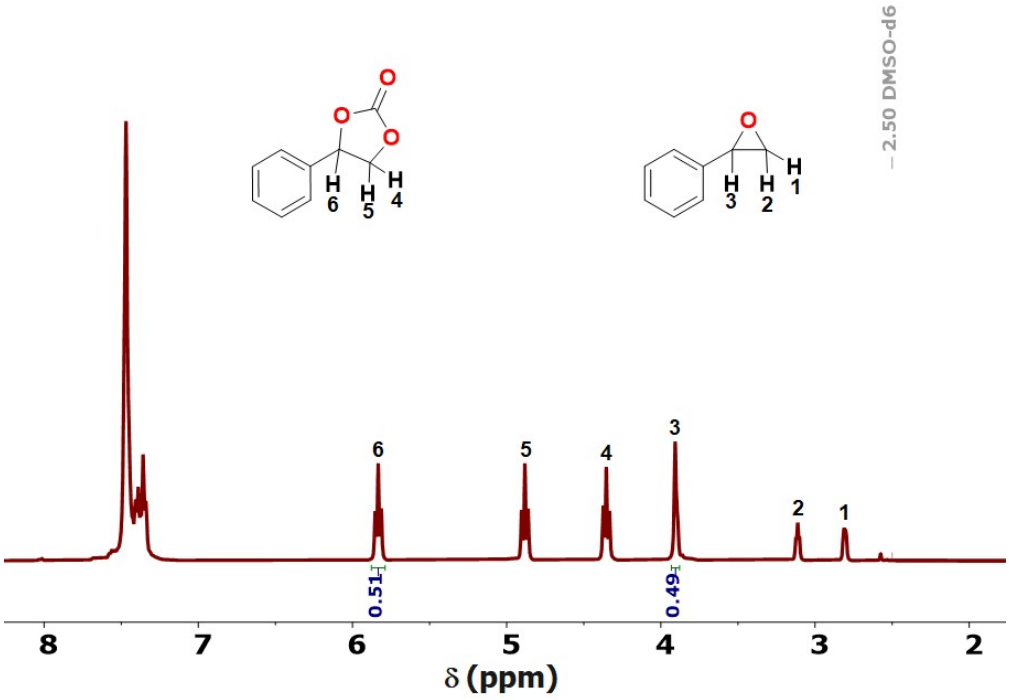

Figure S28. ^{1}H NMR spectrum (measured in DMSO-d_6) of the conversion of SO into the 4-phenyl-1,3-dioxolan-2-one catalyzed by 1 mol% Zn-dtc$_2$ in 0.2 mL DMSO-d_6, 1 atm CO_2 (balloon) and 80 °C for 4 h (Entry 5, Table 2).

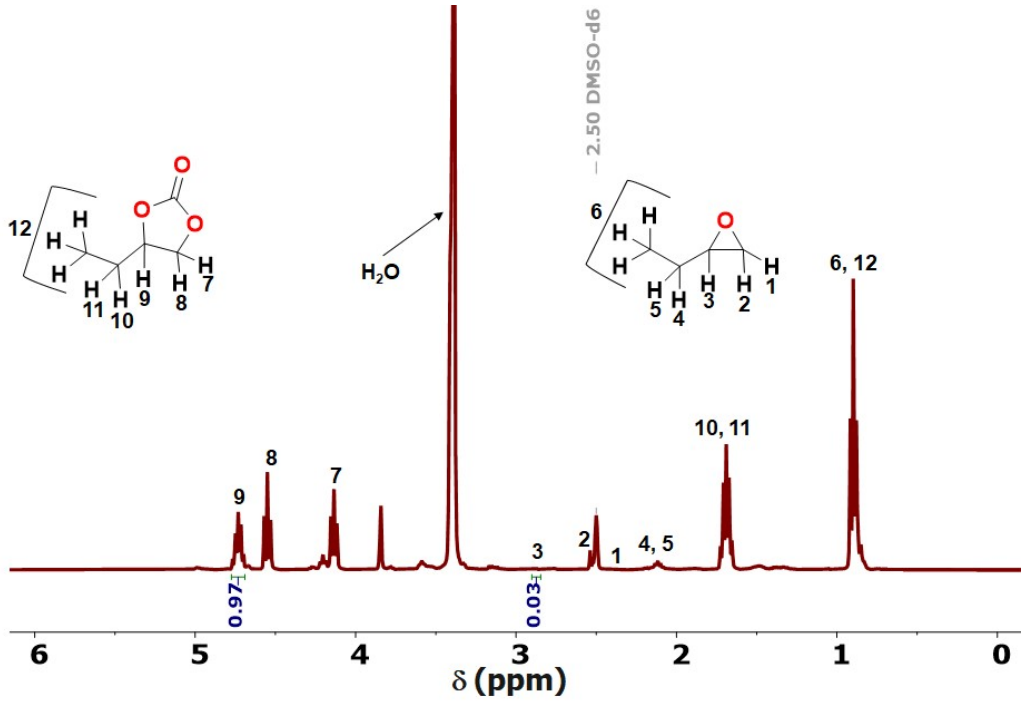

Figure S29. ^{1}H NMR spectrum (measured in DMSO-d_6) of the conversion of BO into the 4-ethyl-1,3-dioxolan-2-one catalyzed by 1 mol% Zn-dtc$_2$ in 0.2 mL DMSO-d_6, 1 atm CO_2 (balloon) and RT for 24 h (Entry 6, Table 2).

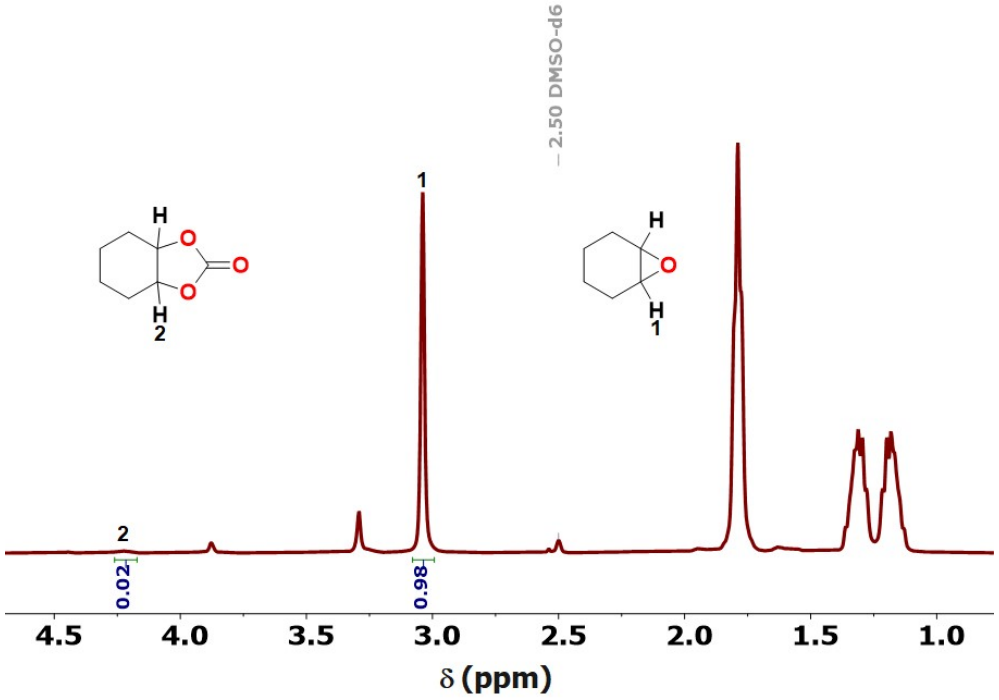

Figure S30. ^{1}H NMR spectrum (measured in DMSO-d_6) of the conversion of CHO into the hexahydrobenzo[d][1,3]dioxol-2-one catalyzed by 1 mol% Zn-dtc$_2$ in neat conditions, 1 atm CO_2 (balloon) and 80 °C for 4 h (Entry 7, Table 2).

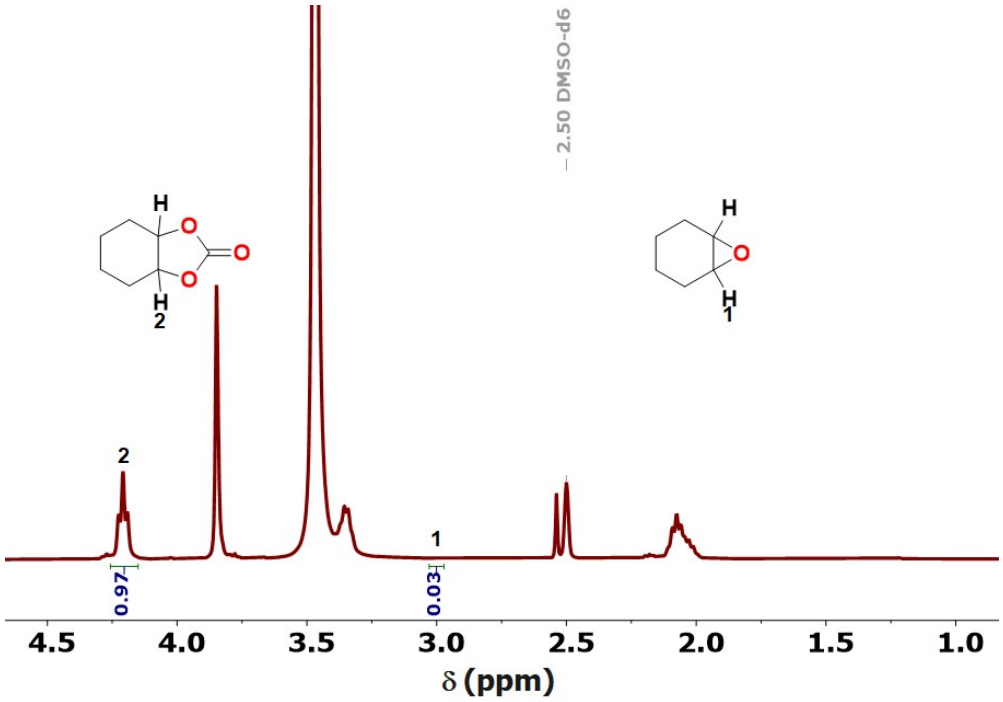

Figure S31. ^{1}H NMR spectrum (measured in DMSO-d_6) of the conversion of CHO into the hexahydrobenzo[d][1,3]dioxol-2-one catalyzed by 1 mol% Zn-dtc$_2$ in 0.2 mL DMSO-d_6, 1 atm CO_2 (balloon) and 80 °C for 4 h (Entry 7, Table 2).

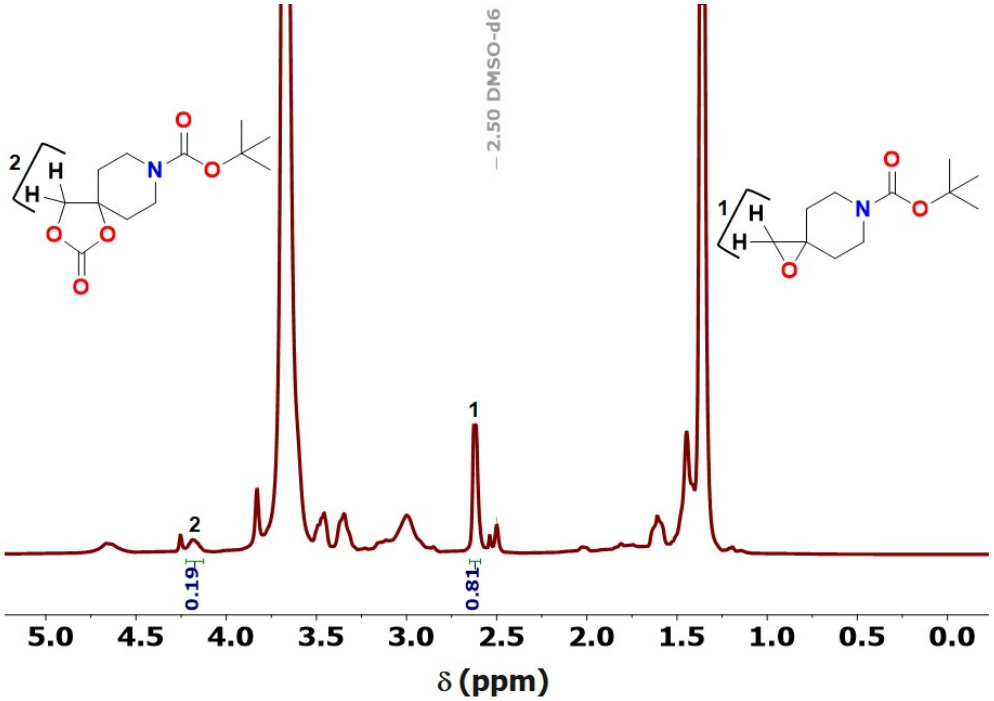

Figure S32. ^{1}H NMR spectrum (measured in DMSO-d_6) of the conversion of TOAC into the *tert*-butyl 2-oxo-1,3-dioxa-8-azaspiro[4.5]decane-8-carboxylate catalyzed by 1 mol% Zn-dtc$_2$ in 0.2 mL DMSO-d_6, 1 atm CO_2 (balloon) and 80 °C for 4 h (Entry 8, Table 2).

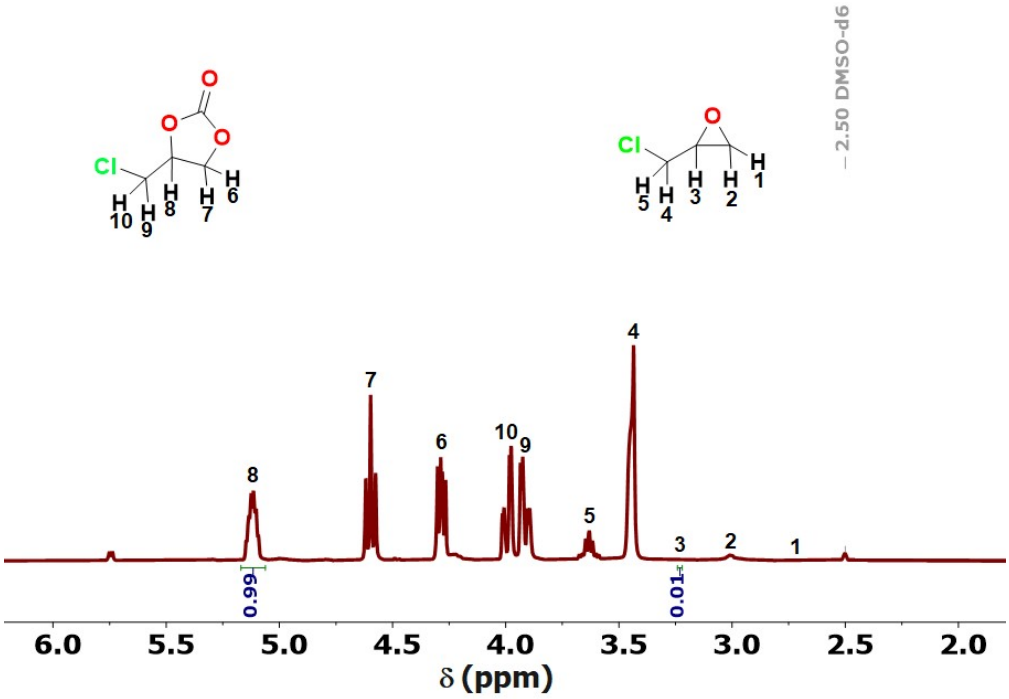

Figure S33. [1]H NMR spectrum (measured in DMSO-d_6) of the conversion of ECH into the 4-chloromethyl-2-oxo-1,3-dioxolane catalyzed by 1 mol% $(Zn\text{-}bdtc)_2$ in 0.2 mL DMSO-d_6, 1 atm CO_2 (balloon) and 80 °C for 4 h (Entry 1, Table 2).

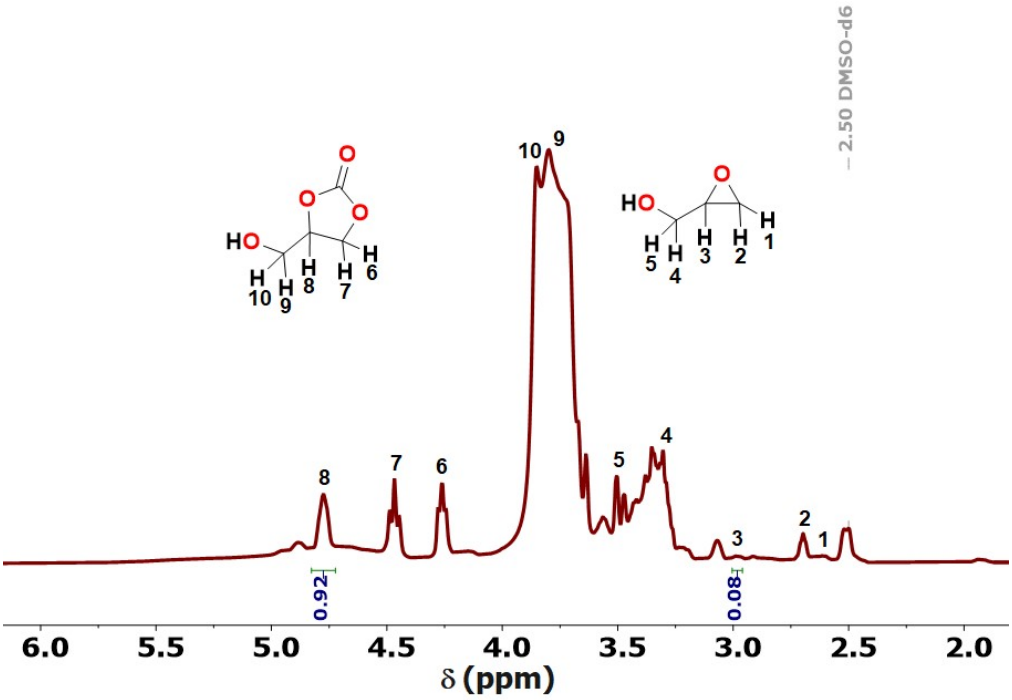

Figure S34. [1]H NMR spectrum (measured in DMSO-d_6) of the conversion of GO into the 4-(hydroxymethyl)-1,3-dioxolan-2-one catalyzed by 1 mol% $(Zn\text{-}bdtc)_2$ in 0.2 mL DMSO-d_6, 1 atm CO_2 (balloon) and 80 °C for 4 h (Entry 2, Table 2).

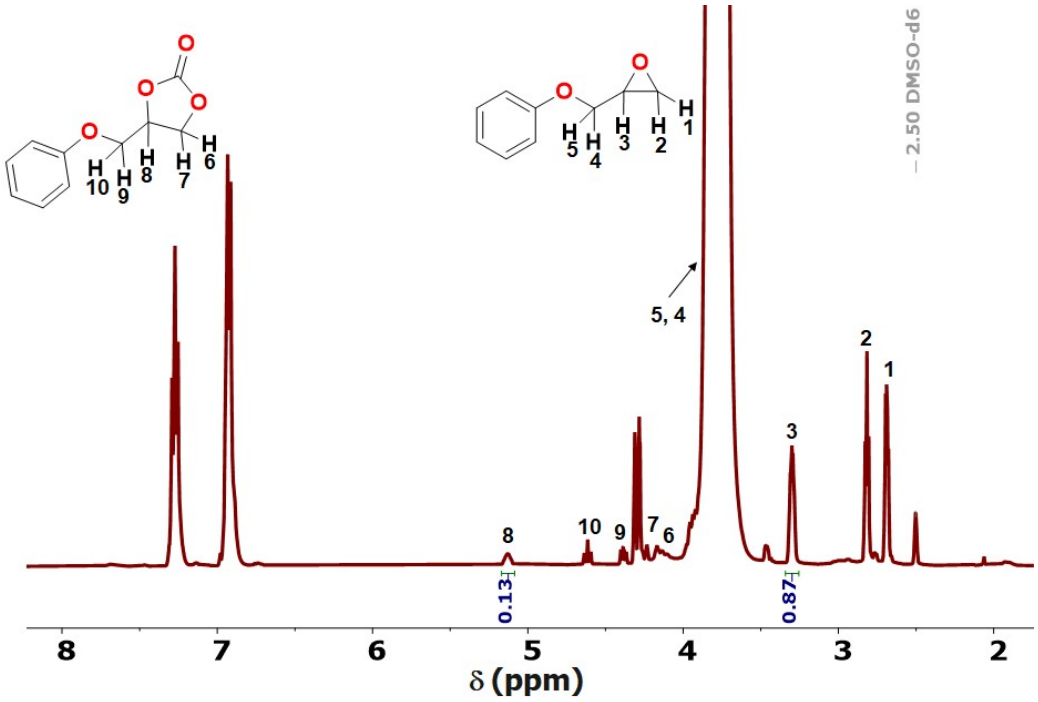

Figure S35. [1]H NMR spectrum (measured in DMSO-d_6) of the conversion of POP into the 4-(phenoxymethyl)-1,3-dioxolan-2-one catalyzed by 1 mol% $(Zn\text{-}bdtc)_2$ in 0.2 mL DMSO-d_6, 1 atm CO_2 (balloon) and 80 °C for 4 h (Entry 3, Table 2).

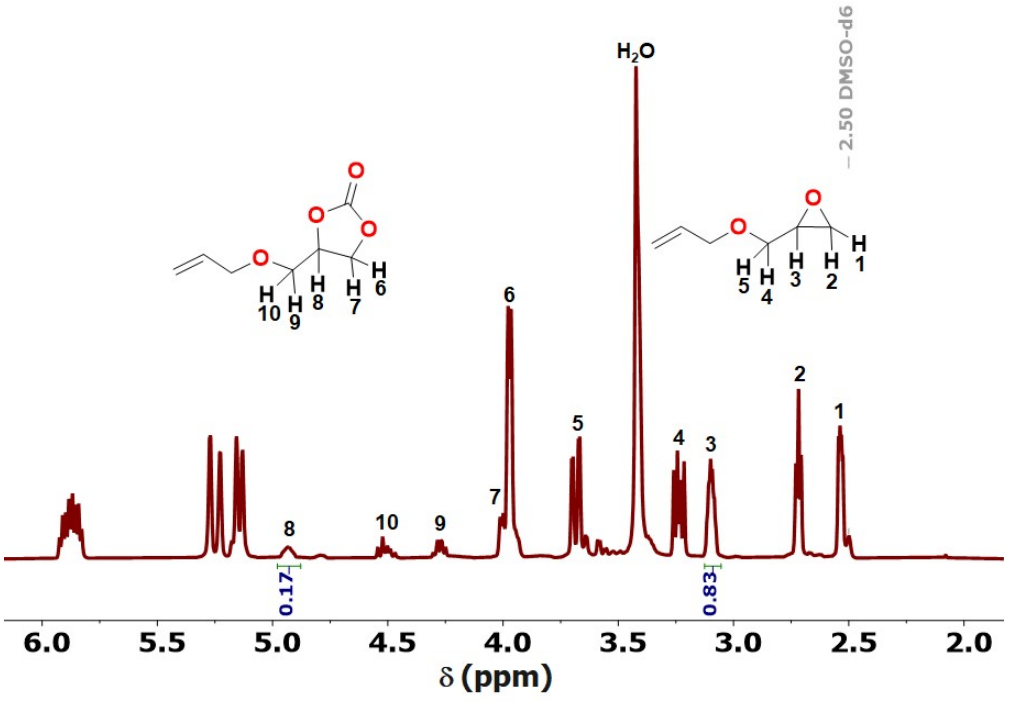

Figure S36. [1]H NMR spectrum (measured in DMSO-d_6) of the conversion of AEG into 4-((allyloxy)methyl)-1,3-dioxolan-2-one catalyzed by 1 mol% $(Zn\text{-}bdtc)_2$ in 0.2 mL DMSO-d_6, 1 atm CO_2 (balloon) and 80 °C for 4 h (Entry 4, Table 2).

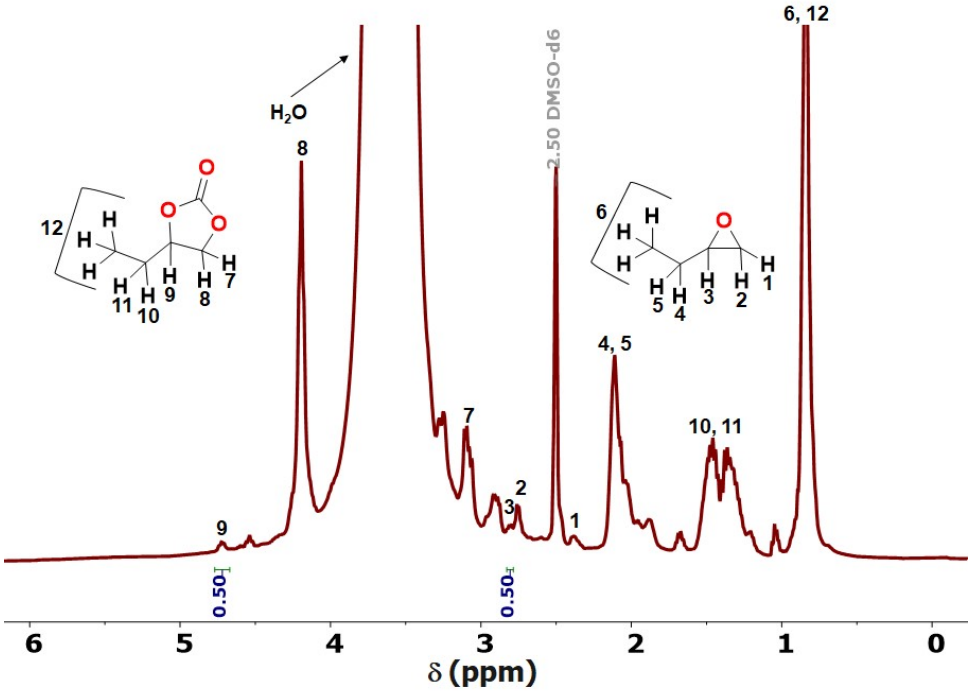

Figure S37. [1]H NMR spectrum (measured in DMSO-d_6) of the conversion of BO into the 4-ethyl-1,3-dioxolan-2-one catalyzed by 1 mol% $(Zn\text{-}bdtc)_2$ in 0.2 mL DMSO-d_6, 1 atm CO_2 (balloon) and RT for 24 h (Entry 5, Table 2).

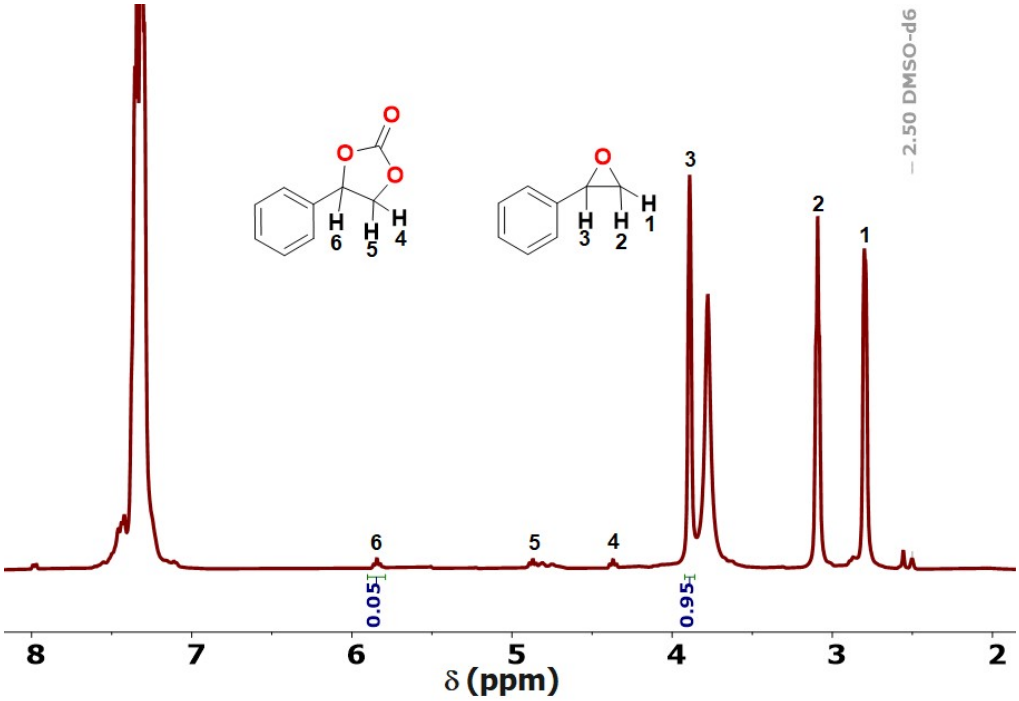

Figure S38. [1]H NMR spectrum (measured in DMSO-d_6) of the conversion of SO into the 4-phenyl-1,3-dioxolan-2-one catalyzed by 1 mol% $(Zn\text{-}bdtc)_2$ in 0.2 mL DMSO-d_6, 1 atm CO_2 (balloon) and 80 °C for 4 h (Entry 6, Table 2).

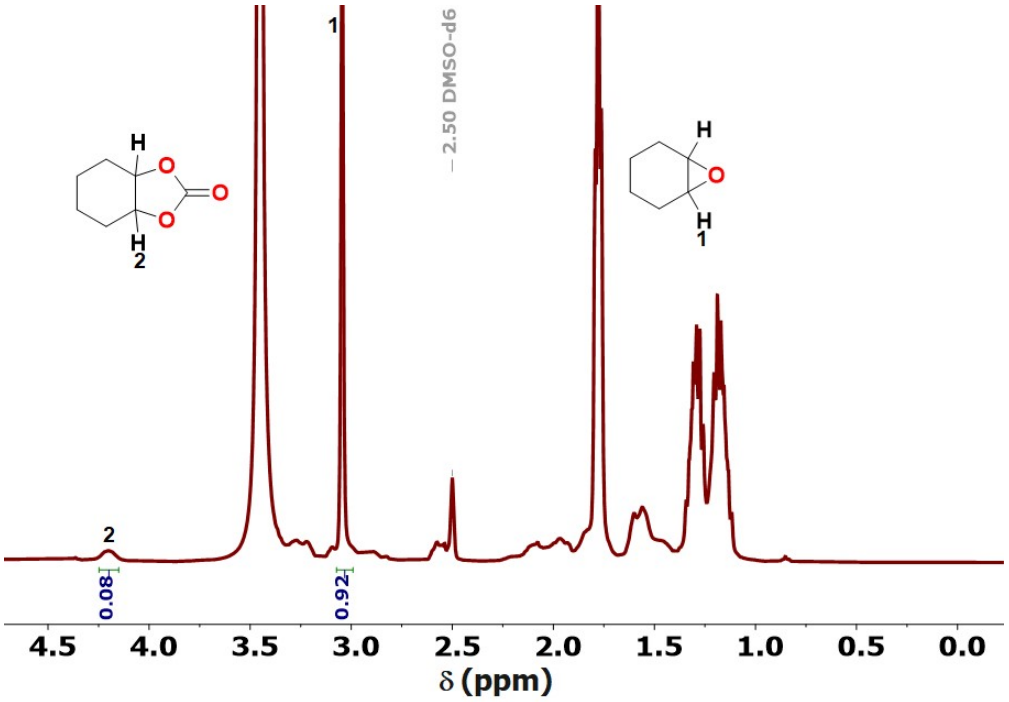

Figure S39. ^{1}H NMR spectrum (measured in DMSO-d_6) of the conversion of CHO into the hexahydrobenzo[d][1,3]dioxol-2-one catalyzed by 1 mol% $(Zn\text{-}bdtc)_2$ in 0.2 mL DMSO-d_6, 1 atm CO_2 (balloon) and 80 °C for 4 h (Entry 7, Table 2).

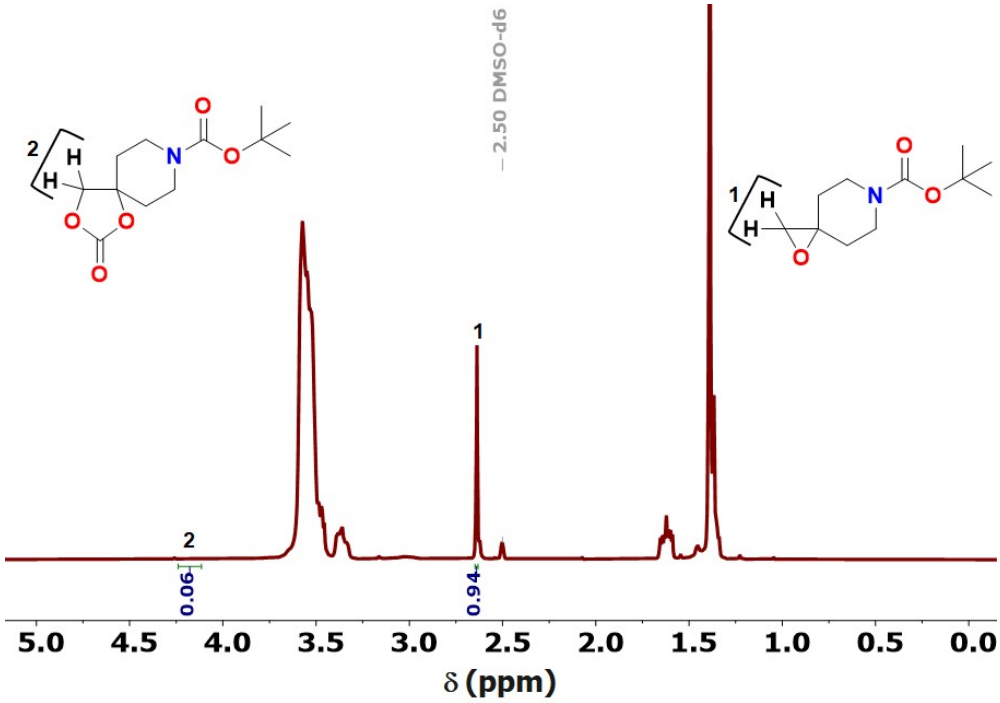

Figure S40. ^{1}H NMR spectrum (measured in DMSO-d_6) of the conversion of TOAC into the *tert*-butyl 2-oxo-1,3-dioxa-8-azaspiro[4.5]decane-8-carboxylate catalyzed by 1 mol% $(Zn\text{-}bdtc)_2$ in 0.2 mL DMSO-d_6, 1 atm CO_2 (balloon) and 80 °C for 4 h (Entry 8, Table 2).

5.3. TON & TOF values

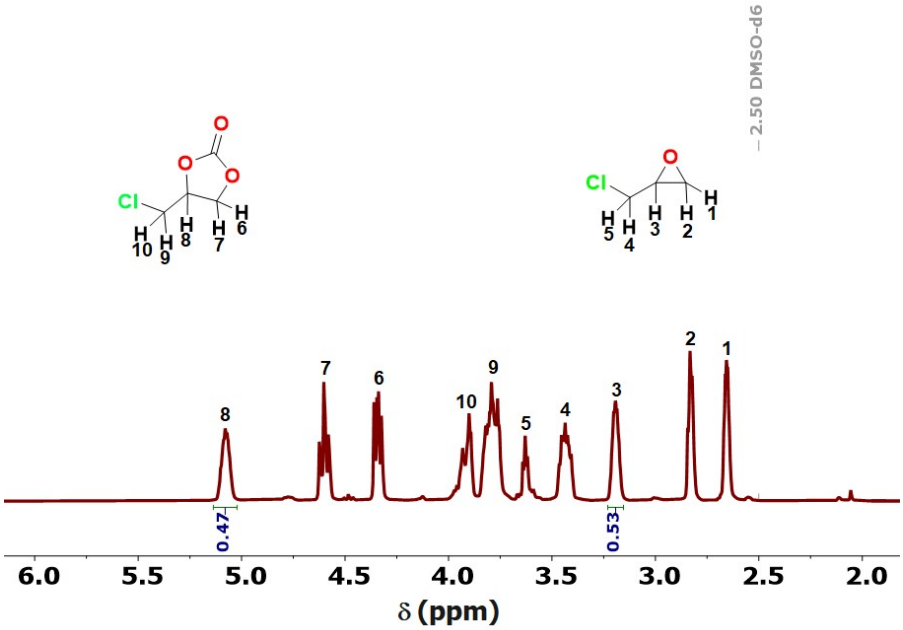

Figure S41. ^{1}H NMR spectrum (measured in DMSO-d_6) of the conversion of ECH into the 4-chloromethyl-2-oxo-1,3-dioxolane catalyzed by 0.1 mol% Zn-dtc$_2$ in 0.2 mL DMSO-d_6, 10 atm CO_2 and 150 °C for 60 min (Entry 1, Table 3).

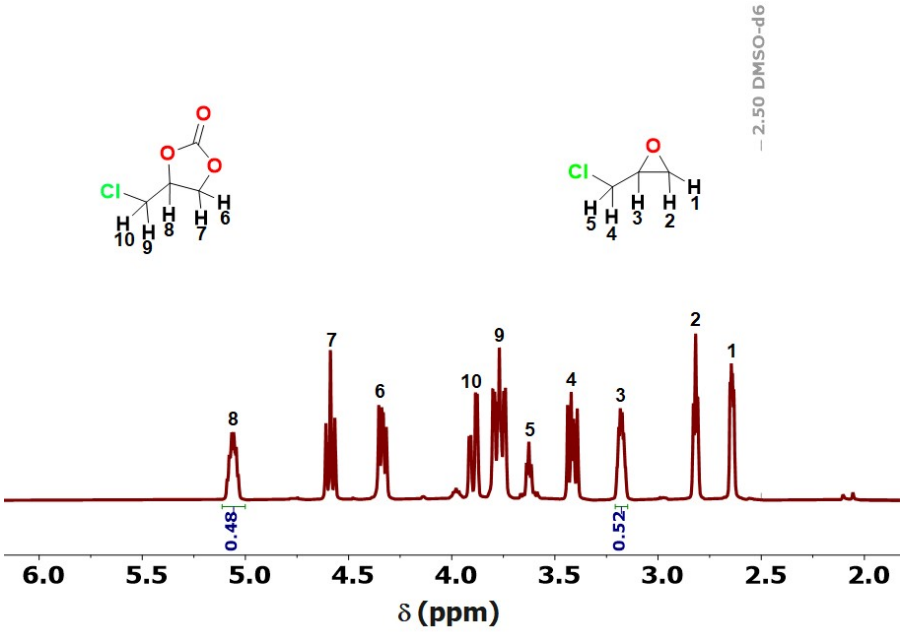

Figure S42. ^{1}H NMR spectrum (measured in DMSO-d_6) of the conversion of ECH into the 4-chloromethyl-2-oxo-1,3-dioxolane catalyzed by 0.05 mol% Zn-dtc$_2$ in 0.2 mL DMSO-d_6, 10 atm CO_2 and 150 °C for 120 min (Entry 2, Table 3).

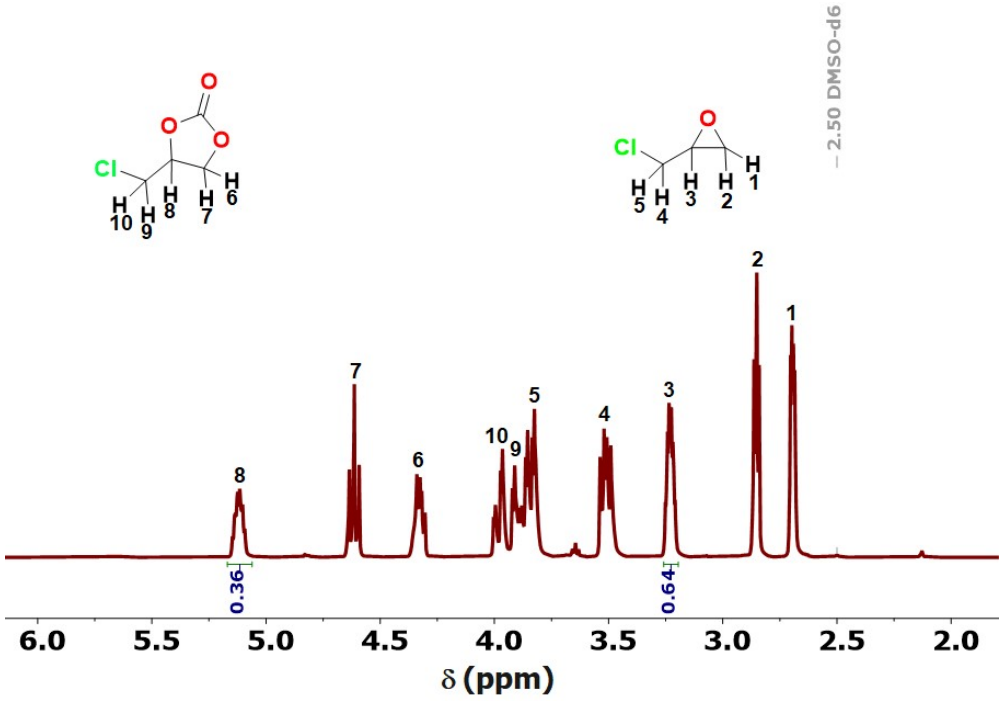

Figure S43. [1]H NMR spectrum (measured in DMSO-d_6) of the conversion of ECH into the 4-chloromethyl-2-oxo-1,3-dioxolane catalyzed by 0.1 mol% Zn-dtc$_2$ in neat conditions, 10 atm CO_2 and 160 °C for 30 min (Entry 3, Table 3).

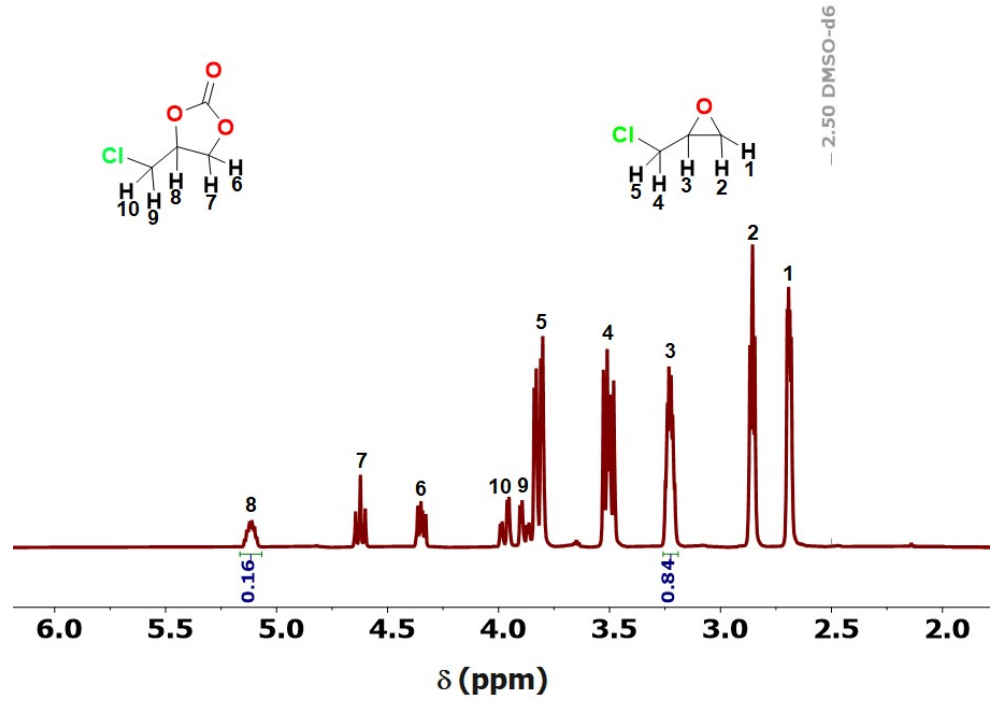

Figure S44. [1]H NMR spectrum (measured in DMSO-d_6) of the conversion of ECH into the 4-chloromethyl-2-oxo-1,3-dioxolane catalyzed by 0.05 mol% Zn-dtc$_2$ in neat conditions, 10 atm CO_2 and 160 °C for 30 min (Entry 4, Table 3).

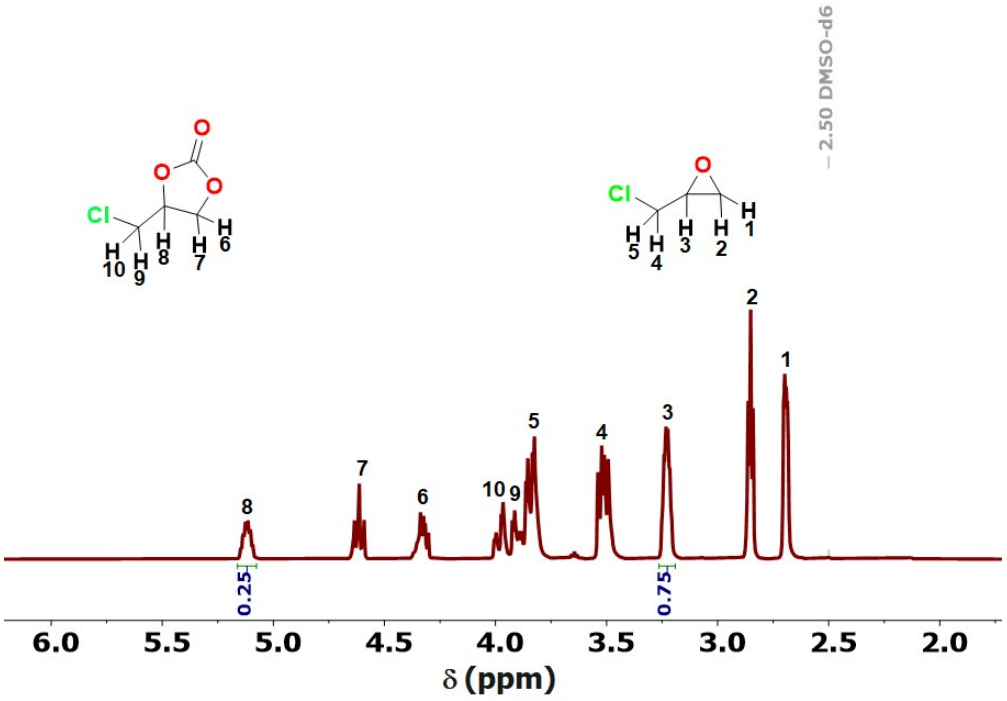

Figure S45. [1]H NMR spectrum (measured in DMSO-d_6) of the conversion of ECH into the 4-chloromethyl-2-oxo-1,3-dioxolane catalyzed by 0.05 mol% Zn-dtc$_2$ in neat conditions, 20 atm CO_2 and 160 °C for 15 min (Entry 5, Table 3).

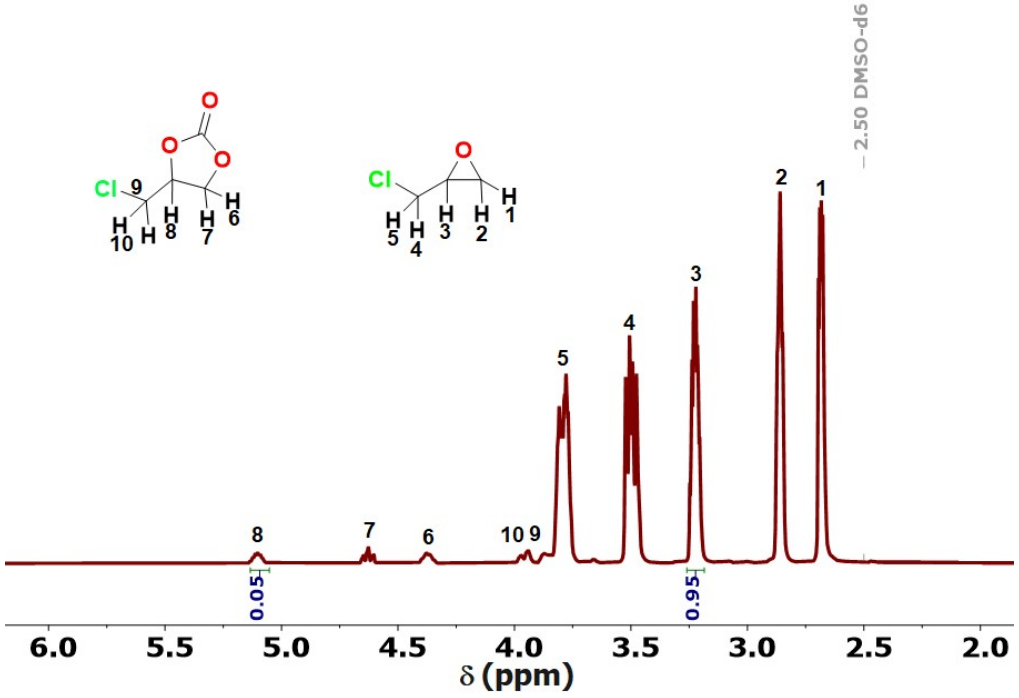

Figure S46. [1]H NMR spectrum (measured in DMSO-d_6) of the conversion of ECH into the 4-chloromethyl-2-oxo-1,3-dioxolane catalyzed by 0.005 mol% Zn-dtc$_2$ in neat conditions, 20 atm CO_2 and 160 °C for 60 min (Entry 6, Table 3).

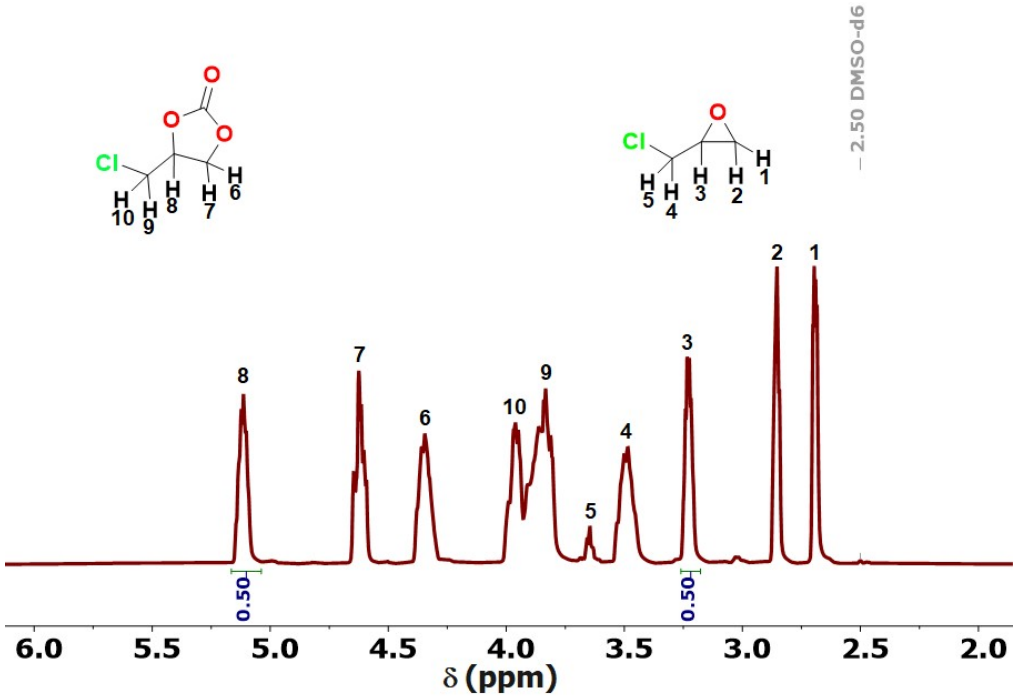

Figure 47. ^{1}H NMR spectrum (measured in DMSO-d_6) of the conversion of ECH into the 4-chloromethyl-2-oxo-1,3-dioxolane catalyzed by 0.1 mol% (Zn-bdtc)$_2$ in neat conditions, 20 atm CO_2 and 160 °C for 30 min (Entry 7, Table 3).

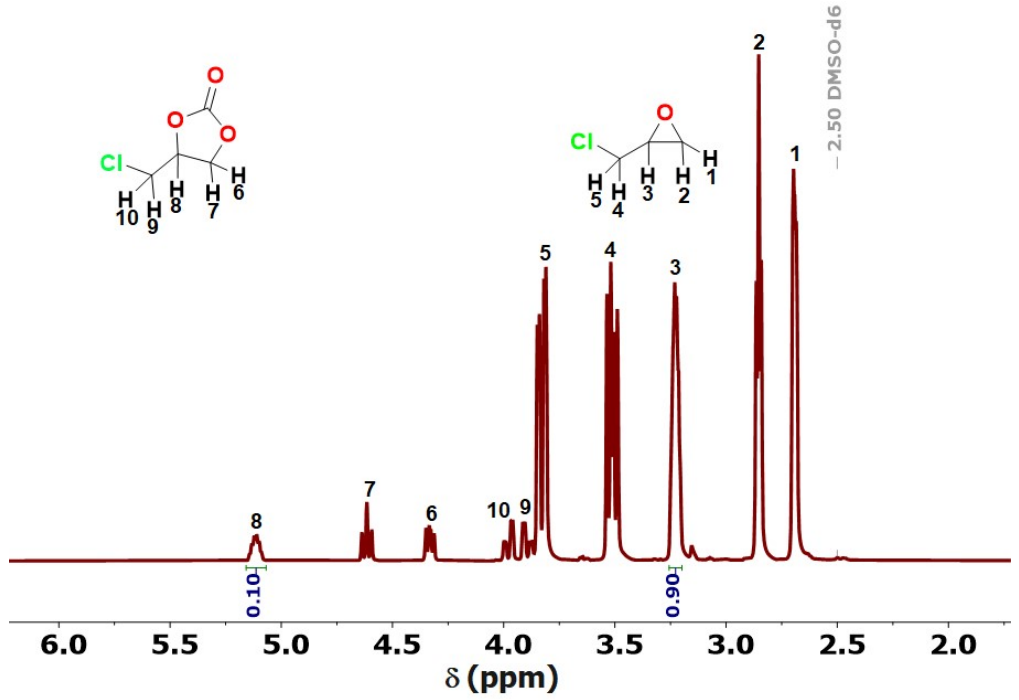

Figure S48. ^{1}H NMR spectrum (measured in DMSO-d_6) of the conversion of ECH into the 4-chloromethyl-2-oxo-1,3-dioxolane catalyzed by 0.005 mol% (Zn-bdtc)$_2$ in neat conditions, 20 atm CO_2 and 160 °C for 60 min (Entry 8, Table 3).

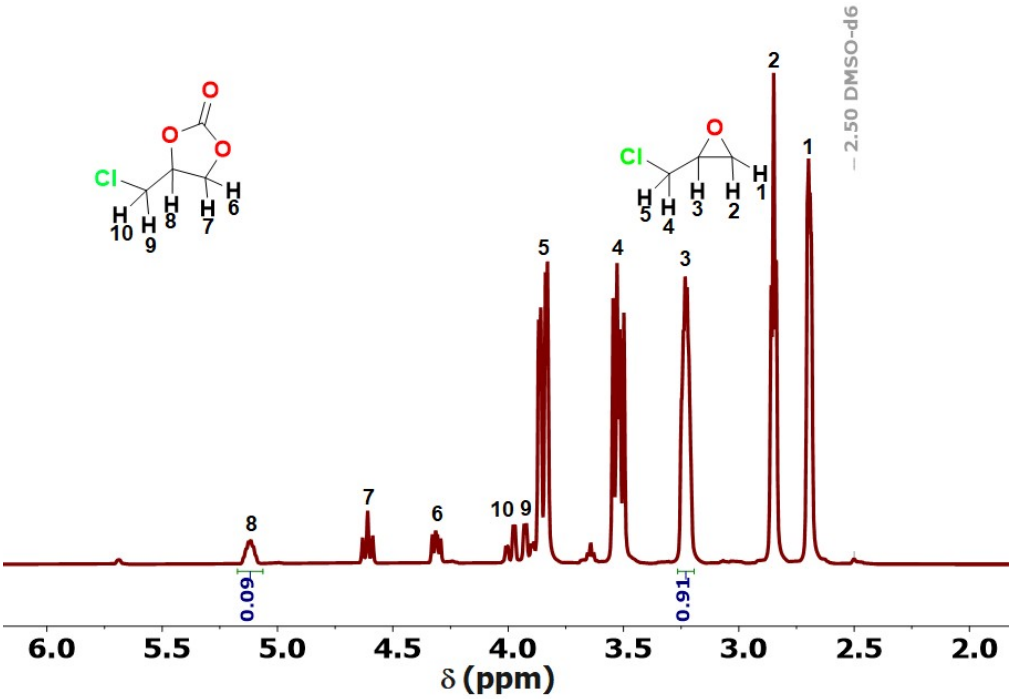

Figure S49. ^{1}H NMR spectrum (measured in DMSO-d_6) of the conversion of ECH into the 4-chloromethyl-2-oxo-1,3-dioxolane catalyzed by 0.1 mol% $(Zn\text{-}bdtc)_2$ in neat conditions, 20 atm CO_2 and 160 °C for 15 min (Entry 9, Table 3).

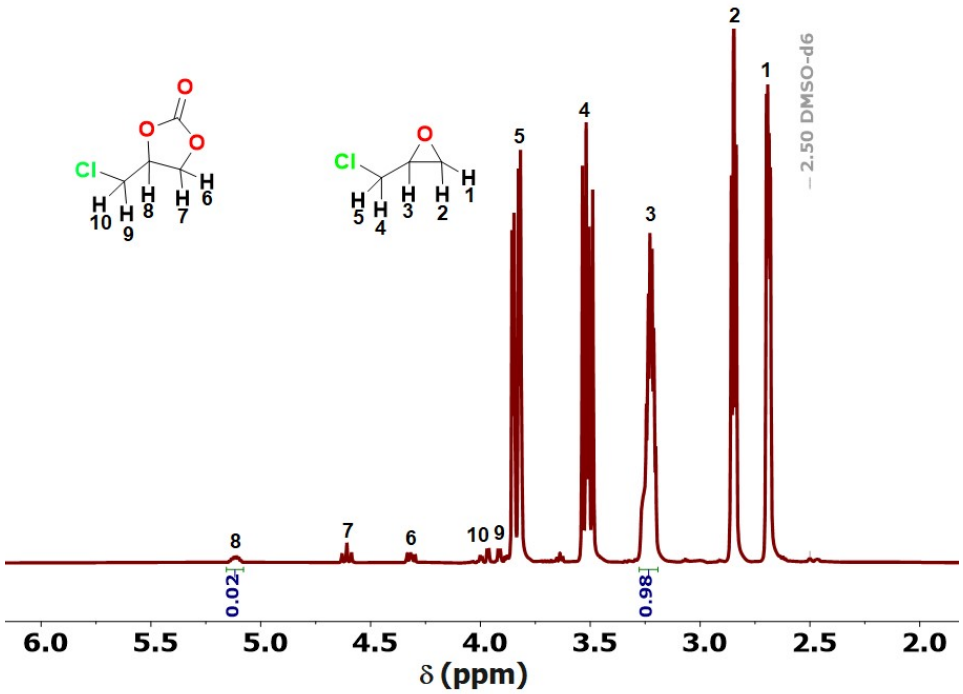

Figure S50. ^{1}H NMR spectrum (measured in DMSO-d_6) of the conversion of ECH into the 4-chloromethyl-2-oxo-1,3-dioxolane catalyzed by 0.05 mol% $(Zn\text{-}bdtc)_2$ in neat conditions, 20 atm CO_2 and 160 °C for 15 min (Entry 10, Table 3).

Table S1. Quantities of catalysts and ECH used in **Table 1**.

Entry	Catalyst	Mass (mg)	ECH volume (mL)
1	$Zn\text{-}dtc_2$	20	0.24
2			0.24
3			0.24
4			0.24
5			0.48
6			0.16
7			0.24
8			0.24
9	$ZnBr_2$	20	0.68
10	dtc	30	0.86
11			0.36

Table S2. Quantities of substrates used with either $Zn\text{-}dtc_2$ (20 mg) or $(Zn\text{-}bdtc)_2$ (10 mg) in **Table 2**.

Epoxide	Volume (mL) used with $Zn\text{-}dtc_2$	Volume (mL) used with $(Zn\text{-}bdtc)_2$
ECH†	0.24	0.08
GO†	0.20	0.07
POP†	0.40	0.14
AGE†	0.36	0.12
SO†	0.35	0.12
BO†	0.26	0.09
CHO†	0.30	0.10
TOAC‡	0.64	0.22

† *The densities of the epoxides (g/mL) are as follows: ECH, 1.183; GO, 1.117; POP, 1.109; AGE, 0.962; SO, 1.054; BO, 0.829; and CHO, 0.970.*
‡ *Note: TOAC is a solid, and its amount is reported in grams.*

Table S3. Quantities of catalysts and ECH used in **Table 3**.

Entry	Catalyst	Mass (mg)	ECH volume (mL)
1	$Zn\text{-}dtc_2$	20.0	2.40
2		20.0	4.80
3		20.0	2.40
4		20.0	4.80
5		20.0	2.40
6		3.0	7.10
7	$(Zn\text{-}bdtc)_2$	10.0	0.80
8		5.0	8.10
9		10.0	0.80
10		10.0	1.60

References

(1) Eftaiha, A. F.; Qaroush, A. K.; Hasan, A. K.; Helal, W.; Al-Qaisi, F. M. CO_2 Fixation into Cyclic Carbonates Catalyzed by Single-Site Aprotic Organocatalysts. *React. Chem. Eng.* **2022**, *7* (8), 1807–1817. https://doi.org/10.1039/D2RE00157H.

(2) Qaroush, A. K.; Eftaiha, A. F.; Al-Qaisi, F. M.; Assaf, K. I.; Hammad, S. B.; Al-Anati, M. H.; Radwan, E. S.; Awwadi, F. F. Newly Synthesized Imidazolium Precursors for CO_2 Utilization and Sequestration: Aprotic *versus* Protic Salts. *Catal. Sci. Technol.* **2023**, *13* (11), 3245–3257. https://doi.org/10.1039/D3CY00270E.